Electrophysiological Mechanisms of Psychedelic Drugs: A Systematic Review

Javier Hidalgo Jiménez[1†], Kristjan Kaup[2], Jaan Aru[2]

[1] Independent Scholar

[2] Institute of Computer Science, University of Tartu, Estonia

[†] Corresponding author

ABSTRACT

Serotonergic psychedelics are known for their profound effects on consciousness and are gaining renewed interest as potential psychiatric treatments. These advances underscore the need to clarify the mechanisms of action of these compounds. This systematic review compiles and critically evaluates 23 *in vitro* and 26 *in vivo* electrophysiological studies on psychedelic compounds, with an emphasis on layer 5 pyramidal neurons in the prefrontal cortex, where 5-HT_{2A} receptors are densely expressed. Our findings reveal that psychedelics exert complex, heterogeneous effects on neuronal excitability, synaptic transmission, and network oscillations. These results challenge the simplified view that psychedelics uniformly increase cortical excitability. Instead, they modulate both excitatory and inhibitory processes in a cell-type- and compartment-specific manner, with evidence for biphasic, dose-dependent, and context-sensitive responses. Activation of 5-HT_{2A} receptors leads to intricate calcium signaling, downregulating excitatory currents and firing rates in many neurons, while enhancing glutamate release and activating a subset of projection fibers. Modulation of presynaptic and extrasynaptic GluN2B-containing NMDA receptors appears central to these effects, and some indirect evidence supports the involvement of intracellular 5-HT_{2A} receptors. These insights prompt a reassessment of prevailing models of psychedelic action and underscore the value of incorporating electrophysiological data into psychedelic neuropharmacology.

Keywords: psychedelics, electrophysiology, 5-HT_{2A}, DOI, LSD, NBOH

1. INTRODUCTION

Psychedelics are a family of tryptamines (e.g., psilocybin), ergolines (e.g., lysergic acid diethylamide, LSD), and phenylethylamines (e.g., 2,5-dimethoxy-4-iodoamphetamine, DOI) that profoundly alter human consciousness. Plant and fungal species containing psychedelic alkaloids grow on all five continents, and evidence of their use dates back to

Neolithic cave paintings (Escohotado, 2005). Their relevance to archaic religions is certain among pre-Columbian civilizations of Central America and the Andes, and possible in the Vedic culture. They were also likely used in the Eleusinian Mysteries for nearly 2,000 years—rites attended by figures such as Plato, Aristotle, Cicero and Marcus Aurelius (Escohotado, 2005; Nichols, 2016). The effects include sensory alterations such as synesthesia and hallucinations, distortions in the perception of space and time, distortions of identity (ego dissolution or ego death), and ecstatic experiences (Nichols, 2016).

Recently, psychiatry has become interested in these drugs. Psychedelics have shown promising results in clinical trials, emerging as potential treatments for psychiatric conditions with high prevalence and morbidity, such as major depression and anxiety (Davis et al., 2021; dos Santos et al., 2018; Goodwin et al., 2022; Muttoni et al., 2019; Raison et al., 2023; Schimmers et al., 2022; von Rotz et al., 2023). Computational neuroscientists have also become interested in modeling the effects of psychedelic drugs on brain dynamics (Deco et al., 2018; Herzog et al., 2023; Irrmischer et al., 2025; Kringelbach et al., 2020; Luppi et al., 2021), in an attempt to better understand brain states.

Psychedelics are partial agonists at the serotonin 2A receptor (5-HT_{2A}). 5-HT_{2A} is a G protein-coupled receptor (GPCR). Through $G\alpha_{q/11}$-mediated signaling, it activates the release of Ca^{2+} from intracellular stores. Ca^{2+} ions activate protein kinases like protein kinase C (PKC) or the Ca^{2+}/calmodulin-dependent protein kinase II (CaM-KII). Protein kinases phosphorylate ionic channels in the cell, modulating excitability. Activation of 5-HT_{2A} has been shown to increase neural excitability (Aghajanian & Marek, 1999). Additionally, psychedelics promote the release of glutamate (Wojtas et al., 2022), further contributing to neuronal excitation.

The receptor is expressed in various cell types across the brain, including both excitatory and inhibitory neurons, as well as glia. However, it is most abundant in the apical dendrites of layer 5 pyramidal (L5p) neurons (Chiu et al., 2023; Weber & Andrade, 2010). Because L5p cells occupy a central position in cortical computations and are highly interconnected with the thalamus, they are considered key to brain function and consciousness (Aru et al., 2020).

Most current approaches to understanding the action of psychedelics rely on resting-state neuroimaging, a field that has seen tremendous advancements. The sophistication of fMRI and the involvement of computational neuroscientists have revolutionized psychedelic science. However, due to the inherent limitations of these methods, it is crucial to validate

and support their findings with more precise physiological techniques, such as electrophysiology. Resting-state fMRI studies, for instance, often interpret increased functional connectivity as heightened neuronal activity (Ghaw et al., 2024). Yet, several studies in humans and rodents have reported a generalized decrease in BOLD signal across the brain during psychedelic states (Carhart-Harris et al., 2012; Ghaw et al., 2024; Riga et al., 2014), despite increased between-network functional connectivity. Since BOLD signal changes can reflect alterations in both inhibitory and excitatory processes, fMRI alone cannot fully disentangle these mechanisms. Electrophysiology, which directly measures neuronal firing rates, oscillatory activity, and synaptic transmission, provides the temporal and physiological precision necessary to clarify how psychedelics modulate neural function. Given these advantages, revisiting electrophysiological research—an area that thrived before the modern "renaissance" of psychedelic science—is essential for complementing and refining insights derived from neuroimaging (Smausz et al., 2022).

Several popular reviews of psychedelic activity overemphasize the excitatory effects of psychedelics (e.g., van Elk and Yaden, 2022; Vollenweider and Preller, 2020), leaving an impression that psychedelics have a neat excitatory action in neurons and circuits. Moreover, several leading hypotheses about the mode of action of psychedelics—often based on neuroimaging—rely on their ability to increase neural activity. For instance, the Relaxed Beliefs Under Psychedelics (REBUS) hypothesis proposes that increased excitability of L5p neurons dysregulates higher-order brain functions, leading to decreased top-down control (Carhart-Harris et al., 2014; Carhart-Harris & Friston, 2019). Similarly, the Cortico-Striato-Thalamo-Cortical (CSTC) loop hypothesis, inspired by classic models of schizophrenia, posits that psychedelic hallucinations arise from heightened excitability in L5p neurons, reducing thalamic inhibition of sensory input (Vollenweider & Geyer, 2001; Vollenweider & Preller, 2020).

Despite some work on psychedelics showing increased neural excitability *in vitro* and *in vivo* (Araneda & Andrade, 1991; De Gregorio et al., 2021; Shao et al., 2025), there is considerable evidence suggesting a significantly more complex picture. For instance, LSD and DOI can reduce neural firing across both excitatory and inhibitory cells in a wide range of cortical and subcortical regions in awake animals (Brys et al., 2023). Moreover, *in vivo* studies show that DOI, which lacks inhibitory 5-HT_{1A} agonist activity, reliably inhibits L5p firing in a dose-dependent manner when applied locally (Ashby et al., 1989; Ashby & Wang, 1990; Bambico et al., 2010; Bergqvist et al., 1999; El Mansari & Blier, 1997, 2005; Rueter & Blier, 1999; Reuter et al., 2000). These often-overlooked findings underscore the

complexity of psychedelic effects on neuronal activity and call for a reassessment of some of the most prevailing concepts in this field of research.

Nevertheless, accessing the literature about electrophysiological research on psychedelics remains challenging. Many results are buried within studies focused on serotonin and its receptors, rather than psychedelics specifically. Additionally, some findings appear contradictory and only make sense after carefully analyzing experimental procedures and comparing work from different authors.

Here we present a systematic review dedicated to the electrophysiological effects of psychedelic drugs. We cover both *in vitro* experiments using cortical slices and *in vivo* studies.

Since 5-HT_{2A} receptors are predominantly expressed in L5p neurons we include only *in vitro* studies that examine pyramidal neurons from layers 5 and 6, as these layers are often mixed in experimental designs. Additionally, because the prefrontal cortex (PFC) is highly enriched in 5-HT_{2A} receptors and is involved in numerous cognitive functions, it has been a primary focus in psychedelic research. Therefore, we include only *in vivo* experiments that record from at least one area of the frontal cortex. Most research has been conducted with DOI, given its relative accessibility and specificity for 5-$HT_{2A/C}$ receptors. Other psychedelic phenylethylamines included in this review are DOB, a bromine-substituted congener of DOI; and TCB-2 and 25CN-NBOH (NBOH), which exhibit high potency and selectivity for the 5-HT_{2A} receptor. We also examine LSD, which has been extensively studied in clinical psychedelic research, as well as psilocin and psilocybin, the active compounds in psychedelic mushrooms that have gained significant interest in clinical applications. Additionally, we include DMT and 5-MeO-DMT, two short-acting psychedelics, along with 4-OH-DiPT, a psilocin derivative.

The first part of the Results section will summarize *in vitro* research. We will begin by presenting the effects of psychedelics on passive membrane properties, such as resting membrane potential (RMP) and input resistance (Ri). Next, we will describe their postsynaptic effects, detailing the complex modulation of excitatory postsynaptic potentials (EPSPs) and currents (EPSCs), their underlying mechanisms, and their peculiar effects on asynchronous EPSCs. Finally, we will examine how psychedelics influence action potential spikes.

The second part of the Results section will focus on *in vivo* experiments. We will start by analyzing the effects of local microiontophoretic drug application on neuronal firing. Then,

we will explore the effects of systemic drug administration in anesthetized animals, addressing both neuronal firing and oscillatory activity. Lastly, we will review *in vivo* experiments in awake animals, covering firing distribution, firing activity, and oscillatory dynamics.

Within sections, the experiments will be addressed in chronological order.

In the discussion, we propose a cohesive framework, inspired by Dendritic Integration Theory (Bachman et al., 2020), to elucidate the electrophysiological effects of psychedelics. We also introduce a unified molecular mechanism of synaptic modulation by psychedelic compounds. Finally, we examine the role of 5-HT_{2A} receptor-mediated neural inhibition in mediating the effects of these substances.

2. METHODS

Data for this systematic review were collected following the systematic reviews and meta-analyses guidelines (Preferred Reporting Items for Systematic Reviews and Meta-Analyses [PRISMA]). The review was not registered.

2.1 Search

PubMed was used to identify relevant articles, with no restrictions on publication dates. Both peer-reviewed articles and preprints were included (see Tables S1 and S2 for details on non-peer-reviewed papers). The final search was performed on 05.12.2025. The following search terms were employed: : ("psychedelic*" OR "hallucinogen*" OR "LSD" OR "psilocybin" OR "psilocin" OR "ayahuasca" OR "DMT" OR "dimethyltryptamine" OR "N,N-dimethyltryptamine" OR "mescaline" OR "DOI" OR "2,5-Dimethoxy-4-iodoamphetamine" OR "DOM" OR "2,5-Dimethoxy-4-methylamphetamine" OR "DOB" OR "2,5-Dimethoxy-4-bromoamphetamine") AND ("electrophysiolog*" OR "neurophysiolog*" OR "cortical slice*" OR "brain slice*" OR "field potential*" OR "neuronal activity" OR "multi-unit recording*" OR "local field potential*" OR "spike train*" OR "neuronal oscillations" OR "patch clamp*" OR "single unit extracellular recording*" OR "microelectrode intracellular recording*") AND ("prefrontal cortex" OR "PFC" OR "medial prefrontal cortex" OR "mPFC" OR "ventromedial prefrontal cortex" OR "vmPFC" OR "dorsolateral prefrontal cortex" OR "dlPFC" OR "orbitofrontal cortex" OR "OFC" OR "pyramidal neuron" OR "pyramidal cell" OR "pyramidal neurons" OR "pyramidal cells") AND ("journal article"[Publication Type] OR "preprint"[Publication Type]) NOT review[Publication Type]. The literature search tagged

both the title and the abstract. An additional search was conducted in Google Scholar to ensure comprehensive coverage of relevant literature.

2.2 Eligibility criteria

Studies were excluded if they met any of the following conditions:

1. They were not original research (e.g., reviews, commentaries, or meta-analyses);
2. The serotonergic agonists used do not produce in animals behavioral responses suggestive of a hallucinogenic effect in humans;
3. They did not assess electrophysiological properties of single layer 5 pyramidal neurons in vitro (such as passive membrane properties, postsynaptic currents or potentials, or action potentials);
4. They did not involve in vivo intracerebral electrophysiological recordings (e.g., single-unit activity, multi-unit activity, or local field potentials);
5. They did not examine at least one region within the frontal cortex.

2.3 Data extraction

After removing duplicates, all remaining articles underwent title and abstract screening. Studies that did not fulfill the eligibility criteria were excluded. Full-text assessments were conducted to determine eligibility.

For each *in vitro* included study, the following data were extracted: (1) specie; (2) recorded region; (3) specific psychedelic compound and (4) used concentration; (5) co-treatments and their concentration; effects on (6) passive membrane properties, (7) postsynaptic activity, and (8) action potential parameters; (9) other relevant findings; and (10) peer-review status.

For each *in vivo* study, the following data were extracted: (1) specie; (2) recorded region; (3) the specific psychedelic compound and (4) administered dose; (5) administration route; (6) anesthesia and co-treatments; effects on (7) neural firing (single unit or multi-unit activity) and (8) local field potentials; (9) other relevant findings; and (10) peer-review status.

Given the difficulty of including the exact number of units recorded for each result, the sample size of the experiments was not systematically extracted.

2.4 Identified studies

A flow diagram illustrating the different phases of the systematic review is presented in Figure 1.

2.5 Study selection

139 references were screened based on titles and abstracts, and 79 records were excluded in screening, leaving 60 potential research papers. Full-text reports of the 60

identified research papers were assessed according to eligibility criteria. The systematic search identified 49 eligible studies in total: 23 *in vitro* studies, and 26 *in vivo* studies. When multiple records referred to the same underlying study (e.g., thesis, preprint, and published article), only the most complete or peer-reviewed version was retained. These duplicates were removed during the deduplication stage or consolidated at the data extraction stage, as appropriate.

3. RESULTS

3.1 In Vitro Studies

Results of *in vitro* studies are compiled in Table 1.

3.1.1 Membrane Properties

3.1.1.1 Resting Membrane Potential

DOB and DOI have been repeatedly shown to produce a slight, often statistically insignificant, depolarization of RMP. The effects are observed after 15–20 minutes of treatment and usually range from 2 to 5 mV (Araneda & Andrade, 1991; Arvanov et al., 1999a; Tanaka & North, 1993). More recent experiments have extended these results to other psychedelics, including TCB-2, NBOH and 4-OH-DiPT (Ekins et al., 2023; Lambe & Aghajanian, 2006; Spindle & Thomas, 2014). Despite being small, this effect is sustained in time, persisting after washout periods of up to 100 minutes (Lambe & Aghajanian, 2006). Moreover, the 5-$HT_{2A/C}$ antagonist ketanserin can prevent RMP depolarization (Araneda & Andrade, 1991).

The effect on RMP depends on the L5p neuron population and the developmental stage. In rats aged 2–3 weeks, DOB significantly increased RMP in 50% of L5p neurons in rat mPFC. This effect was blocked by 5-HT_{2A} antagonists a selective 5-HT_{2C} antagonist. After postnatal day 14 (P14), there was a significant reduction in the fraction of cells responding to DOB and the amplitude of their response. Single-cell RT-qPCR in L5p neurons during P6–P15 suggests that the decrease of DOB's depolarizing action cannot be fully explained by a reduction in 5-HT_{2A} expression, suggesting indirect mechanisms acting early in development (Béïque et al., 2004).

3.1.1.2 Input Resistance

The reports about the effect of psychedelic drugs on Ri of L5p neurons are not consistent.

In the rat, DOB has a non-significant concentration-dependent biphasic effect, with Ri increasing at 0.1 µM and decreasing at 20 µM (Arvanov et al., 1999a). After a 15-minute perfusion of 3 µM DOI and a 5–100 minute washout period, Ri increased non-significantly (Lambe & Aghajanian, 2006). Additionally, non-significant DOI-dependent Ri increase has been observed in rat pups (Béïque et al., 2004).

In the mouse, Spindle and Thomas (2014) observed a significant Ri increase of 15 MΩ in mPFC slices treated with TCB-2. Conversely, Ekins et al. (2023) have reported significant Ri decreases by NBOH, 4-OH-DiPT, or DOI. The latter study observed an inverse concentration-dependent effect of NBOH: at lower concentrations (0.1–10 µM), NBOH significantly reduced Ri to a greater extent (-42% to -34%) than at 100 µM (-12%). Similarly, 10 µM 4-OH-DiPT reduced Ri by 27%, while 100 µM increased it by 8%. In contrast, 10 µM DOI reduced Ri by 13%, whereas 100 µM further reduced it by 41%. Anyway, since these drugs have binding affinities for 5-HT_{2A} in the nanomolar range, concentrations of 100 µM are well above in vivo or clinically relevant levels, risking the activation of off-target receptors (for instance, 100 µM NBOH is approximately 450,000 times its binding affinity to 5-HT_{2A}) (Poulie et al., 2020).

3.1.1.3 Other Parameters

In mouse mPFC slices, DOI decreased the holding current by 52 pA, and increased membrane conductance by 1 nS, in most cell recorded (Troca-Marín & Geijo-Barrientos, 2010). Membrane time constant and input capacitance were not consistently affected by NBOH, 4-OH-DiPT, or DOI in a way that reflected any pattern dependent on the drug or its concentration. Additionally, no significant changes in RMP, Ri, input capacitance, or time constant were observed in mouse mPFC slices obtained 48–72 hours after *in vivo* administration of 2 mg/kg DOI (i.p.) (Ekins et al., 2023).

One study evaluating the effects of psilocin on L5p spontaneous firing rates in mouse cortical slices found no significant differences in membrane resistance, capacitance, or time constant between neurons that were excited, inhibited, or unaffected by psilocin (Schmitz et al., 2022).

In summary, psychedelics induce slight but consistent depolarization of the RMP. This effect is sustained over time and depends on 5-$HT_{2A/C}$ receptors. The impact of psychedelics on RMP varies with neuronal population and developmental stage, with younger rats showing stronger responses. Reports on input resistance (Ri) are inconsistent. While some studies indicate a biphasic or slight increase in Ri, others report significant decreases. Other membrane properties, such as capacitance and time

constant, neither show consistent changes across studies. Additionally, *in vivo* administration of DOI does not appear to induce lasting effects on RMP, Ri, or other parameters.

3.1.2 Synaptic Activity

3.1.2.1 Biphasic Modulation of Evoked Excitatory Currents

DOB had a biphasic effect on the EPSCs elicited by N-methyl-D-aspartate (NMDA) in rat mPFC slices, co-treated with tetrodotoxin (TTX; a Na^+ voltage-gated channel inhibitor that prevents action potentials), bicuculline (a $GABA_A$ antagonist), and glycine (that potentiates the conductance of NMDA receptor, NMDAR) (Arvanov et al., 1999a).

At concentrations ranging from 0.01–1 μM, DOB elicited a dose and time-dependent facilitation of NMDA-evoked EPSCs (eEPSC). Currents enhanced by 0.1 μM DOB returned to baseline after a 15-60-minute washing period. A second application of 0.1 μM DOB after the washing period was ineffective. Continuous perfusion with 0.1 μM DOB for 20 minutes inhibited NMDA currents, indicating strong desensitization to the facilitatory effect that lasted more than 1.5 hours. At 20 μM, DOB blocked NMDA eEPSC. No desensitization to the inhibitory action of 20 μM DOB was observed after 30–45 minutes of continuous perfusion (Arvanov et al., 1999a).

Loading MK-801 (an open channel NMDAR antagonist) into the recording pipette selectively blocks postsynaptic NMDARs, while allowing the function of extrasynaptic and presynaptic NMDARs (McKay et al., 2013). Using MK-801-loaded pipettes, 0.1 μM DOB enhanced the facilitatory action of NMDA on eEPSC evoked by the forceps minor's stimulation. At 20 μM, DOB suppressed basal EPSCs and abolished NMDA's facilitatory action. Further pharmacological manipulations to selectively block pre- or postsynaptic calcium signaling, IP3-dependent Ca^{2+} release, PKC, CaM-KII, glutamate release, and non-NMDAR-mediated excitatory currents revealed that the facilitatory effect was likely driven by a presynaptic mechanism. This mechanism involves PKC-mediated potentiation of presynaptic NMDARs by $5\text{-}HT_{2A}$, which increases presynaptic Ca^{2+} levels and facilitates glutamate release. Conversely, the inhibitory effect was attributed to the modulation of postsynaptic NMDARs by $5\text{-}HT_{2A}$, mediated by CaM-KII (Arvanov et al., 1999a).

Both the facilitatory and inhibitory effects on eEPSCs were blocked by $5\text{-}HT_{2A}$ antagonists. Blocking AMPA and kainate receptors (AMPAR/KAR) prevented the facilitatory action and unmasked an inhibitory effect of 1 μM DOB. Additionally, the eEPSC were not affected by

5-HT_{1A} antagonism, 5-HT_3 antagonism, $GABA_B$ antagonism, or by altering glycine concentrations (Arvanov et al., 1999a).

In rat mPFC slices co-treated with TTX, glycine, bicuculline, and a $GABA_B$ antagonist, LSD (0.5–1000 nM) invariably inhibited NMDA-evoked currents (Arvanov et al., 1999b). The onset of this effect required 10 minutes of continuous perfusion and was blocked by 5-HT_{2A} antagonists, or CaM-KII inhibitors, but not a PKC inhibitor. In the presence of a 5-HT_{1A} antagonist, LSD facilitated NMDA eEPSC at high concentrations, an effect that disappeared after 20 minutes and was also blocked by 5-HT_{2A} antagonism. AMPAR/KAR antagonism abolished the facilitatory action of high doses, unmasking an inhibitory effect. Lisuride, a non-hallucinogenic analog of LSD, produced an invariant facilitatory effect under the same conditions (Arvanov et al., 1999b).

In the presence of an AMPAR/KAR antagonist and at a holding potential of -40 mV, which allows the isolation of postsynaptic NMDAR currents, LSD, DOB, and 5-HT reduced the peak amplitude of EPSCs evoked by electrical stimulation of the forceps minor (Arvanov et al., 1999b). The psychoactive potency of LSD, DOB, and 5-HT correlated with their IC_{50} values for inhibiting NMDAR currents: LSD (9 nM) > DOB (130 nM) > 5-HT (31 μM). Moreover, LSD's IC_{50} aligns with its peak plasma levels in humans. Therefore, the researchers hypothesized that the inhibitory action on NMDAR currents is linked to the hallucinogenic effects of psychedelics (Arvanov et al., 1999b).

Notably, one study found that 10 μM DOI decreased the peak amplitude of eEPSCs elicited by electrical stimulation of the corpus callosum in half of the neurons tested (Troca-Marín & Barrientos, 2010). The effect was prevented by selective 5-HT_{2A} receptor antagonism. Moreover, it was reversed after 7–9 minutes of washout, and both the coefficient of variation of amplitude fluctuations and paired-pulse ratios suggested the involvement of a presynaptic mechanism (Troca-Marín & Barrientos, 2010). Therefore, some fibers may also elicit inhibitory actions during the early phase of psychedelic modulation. Nevertheless, L5p neurons were not isolated from other layer neurons in this assay.

3.1.2.2 Mechanisms of EPSC Modulation

When NMDAR currents were non-selectively isolated in mouse mPFC slices, DOI (1 μM, 20 min) significantly increased the amplitude of EPSCs evoked by the electrical stimulation of L1 (Barre et al., 2016). This effect was rapidly reversible upon washout, absent in 5-HT_{2A} knockout (KO) mice, and blocked by ketanserin or ifenprodil, a selective antagonist of NMDARs containing GluN2B subunit. By contrast, when postsynaptic NMDAR currents

were selectively isolated, DOI's facilitatory effect was lost. Moreover, DOI decreased the paired-pulse ratio, suggesting increased presynaptic glutamate release, and, in 5-HT_{2A} KO mice, selectively restoring 5-HT_{2A} expression in thalamic nuclei targeting L5p neurons rescues the facilitatory action (Barre et al., 2016). These results support the hypothesis of psychedelics facilitating NMDAR currents through a presynaptic mechanism (Arvanov et al., 1999a).

In further agreement with Arvanov et al. (1999a), the presynaptic mechanism involved the activation of PKC. Non-selective application of PKC and PLC inhibitors blocked DOI's facilitation, whereas postsynaptic delivery of G-protein inhibitor or PLC inhibitors had no effect. The potentiation was associated with the phosphorylation of Ser1303 in GluN2B subunits of NMDAR, which increased the receptor's conductance and was absent in 5-HT_{2A} KO mice (Barre et al., 2016). However, unlike Arvanov et al. (1999a) findings, DOI's facilitatory action did not desensitize after 20 minutes as long as postsynaptic Ca^{2+} levels remained high and postsynaptic PKC was not inhibited (Barre et al., 2016).

In a follow-up study, researchers isolated AMPAR currents by increasing Mg^{2+} levels and holding L5p neurons at -60 mV. DOI (1 μM, 20 min) decreased the amplitude of AMPAR EPSCs evoked by L1 electrical stimulation (Berthoux et al., 2019). The effect lasted more than 50 minutes. Shorter treatments (2.5 min) produced a transient effect that dissipated after a few minutes. AMPAR inhibition was blocked by 5-HT_{2A} antagonists or a PKC inhibitor, was unaffected by an NMDAR antagonist, and absent in 5-HT_{2A} KO mice. Restoring postsynaptic 5-HT_{2A} expression in L5p neurons rescued the effect. DOI's action was abolished by postsynaptic PKC inhibition (Berthoux et al., 2019). Again, these results align with some of the observations of Arvanov et al. (1999a): the inhibition of eEPSC involved a slow-onset, long-lasting, and postsynaptic mechanism. However, there are some differences, too. The inhibition of AMPAR currents involved postsynaptic PKC activity, whereas the inhibition of NMDAR currents depended on postsynaptic CaM-KII.

The modulation of AMPAR currents involved the receptor's internalization. Electrically induced long-term depression (LTD), that is mediated by postsynaptic AMPAR internalization, occluded DOI's effect and vice versa (Berthoux et al., 2019). Introducing an interfering peptide to block the interaction between the AMPAR subunit GluA2 and the AP2 clathrin adaptor complex—thereby preventing AMPAR internalization—abolished both LTD and DOI's inhibitory effect. The internalization was associated with the phosphorylation of Ser880 on GluA2 (Berthoux et al., 2019).

3.1.2.3 Late eEPSC

Application of DOI (3 μM, 15 min) or LSD (10 nM, 10 min) to rat mPFC slices induced a late, prolonged (up to 2 s) component in eEPSC (Aghajanian & Marek, 1999; Lambe & Aghajanian, 2006, 2007; Stutzmann et al., 2001). This late eEPSC is observed upon electrical stimulation of the forceps minor or the cortical midlayer, at intervals of 10 seconds or more (<0.1 Hz). It is reduced at shorter stimulation intervals and is completely suppressed at intervals of 1 second (1 Hz) (Aghajanian & Marek, 1999; Lambe & Aghajanian, 2006). Late eEPSC remains observable for more than 2 hours after drug washout. In the absence of psychedelics, the late eEPSC occurs only occasionally, appearing in the first 10 sweeps, it has a shorter duration and is more likely to manifest at intervals of 20–30 seconds (Lambe & Aghajanian, 2006).

This mode, in which dendrites generate a prolonged depolarization after eEPSC, corresponds to up states, which are driven by network activity (Lambe & Aghajanian, 2007). Up and down states are dendritic slow oscillations (~1 Hz) between two membrane potentials that are determined by the precise balance of excitation and inhibition (E/I) (Larkum, 2022). When a neuron enters the up state (naturally or after psychedelics), the late eEPSC is not smooth but instead contains gamma-band oscillations (30–80 Hz) nested within the larger eEPSC waveform (Lambe & Aghajanian, 2007).

Interestingly, 5-HT does not induce late eEPSC and, at 100 μM, it suppressed the late component elicited by DOI. The late eEPSC was suppressed by 5-HT_{2A}, non-selective NMDAR and GluN2B-NMDAR antagonist, and by adenosine 1 and D1/5 receptor agonists. The A1 receptor antagonist DPCPX reversed the effects of adenosine. AMPAR/KAR antagonism suppressed both the early and late components of eEPSCs. Lowering Mg^{2+} and Ca^{2+} concentrations from 2 to 1 mM, which enhanced glutamate transmission, elicited spontaneous late EPSCs in the presence of DOI (Aghajanian & Marek, 1999; Lambe & Aghajanian, 2006, 2007; Stutzmann et al., 2001).

Lambe and Aghajanian (2006) hypothesized that glutamate spillover and the asynchronous activation of extrasynaptic GluN2B-containing NMDARs underlie late EPSCs. Supporting their hypothesis, they found that increasing medium viscosity by washing in 5% dextran to hinder glutamate diffusion attenuates the late eEPSC without affecting the early component. Blocking postsynaptic NMDAR by delivering MK-801 through the recording pipette did not prevent the late EPSC. Moreover, inhibiting the excitatory amino acid transporter, which increased glutamate spillover, combined with an mGlu II antagonist to block the autoinhibition of glutamate release, robustly enhanced the

emergence of late EPSCs in the absence of DOI, despite the mGlu II antagonist did not potentiate DOI-dependent late eEPSC.

3.1.2.4 Spontaneous and Miniature Postsynaptic Currents

In rat mPFC slices, DOI increased the frequency of spontaneous EPSCs (sEPSC) in L5p neurons. However, the increase was only 10% of that elicited by 5-HT (Aghajanian & Marek, 1997, 1999). In mouse mPFC slices, focal application of psilocin or NBOH to 5-HT_{2A}-GFP-tagged neurons did not produce significant changes in sEPSC or spontaneous inhibitory postsynaptic currents (sIPSC) (Schmitz et al., 2022). A bath application of NBOH was neither effective in changing sIPSC frequency nor amplitude (Wang et al., 2025).

One preprint showed that DOI or NBOH elicited significant increases in sEPSC frequency only at high or very high concentrations (10–100 µM). Similarly, 4-OH-DiPT increased sEPSC frequency significantly only at 100 µM. The 5-$HT_{2A/C}$ antagonist ketanserin blocked the action of NBOH, while XE-991, a K_v7 channel inhibitor, had no effect (Ekins et al., 2023). They found a significantly greater increase in sEPSC frequency upon bath application of NBOH compared to intracellular drug delivery, suggesting extracellular 5-HT_{2A}-mediation (Ekins et al., 2023). Similar results were reported in a recent peer-reviewed article, where NBOH failed to alter the frequency or amplitude of sEPSCs at 200 nM, but enhanced their frequency at 10 µM (Wang et al., 2025). This effect persisted 30 minutes after washout, but, notably, was lost when the slices were incubated with the drug for 1 hour. The effect was blocked by selective 5-HT_{2A} receptor antagonism (Wang et al., 2025).

However, psychedelics of the NBOMe class, including NBOH, exhibit extremely high affinity for the 5-HT_{2A} receptor. At concentrations far exceeding the nanomolar range, these compounds also act on other serotonin receptors and receptors of a different class, like adrenergic receptors (Poulie et al., 2020). Therefore, the results of Ekins et al (2023) and Wang et al. (2025) might not be relevant *in vivo*.

Miniature EPSCs (mEPSC) were neither significantly affected by the focal application of psilocin nor NBOH (Schmitz et al., 2022). In contrast, a bath application of DOI increased the frequency of AMPAR mEPSC (Barre et al., 2016). The effect was abolished in a high Mg^{2+} (4 mM) medium or after a bath application of an NMDAR antagonist. The increase in mEPSC was likely due to increased presynaptic glutamate release (Barre et al., 2016).

In mPFC slices obtained from rats treated with systemic DMT 24 hours prior to sample collection, an increase in both frequency and amplitude of sEPSCs was observed (Ly et

al., 2018). Similarly, in mPFC slices from mice treated with psilocybin 24 hours prior to sample collection, an increase in frequency and a trend toward increased amplitude ($p = 0.06$) of mEPSCs was seen (Shao et al., 2021). These late increases in sEPSC and mEPSC were attributed to dendritic plasticity and synaptogenesis, rather than to direct electrophysiological action (Ly et al., 2018; Shao et al., 2021).

3.1.2.5 Excitatory Postsynaptic Potentials

In L5p neurons, DOI (3–10 μM) increased the amplitude of evoked EPSPs (eEPSP) elicited by electrical stimulation of Layer 1 (L1) (Aghajanian & Marek, 1997). At 3 μM, DOI increased the amplitude of eEPSP by 30% following L5 electrical stimulation (Zhai et al., 2003). This effect could be abolished by the metabotropic glutamate receptor II (mGlu II) agonist LY379268. In turn, the action of LY379268 was blocked by a mGlu II antagonist (Zhai et al., 2003). By contrast, at 10 μM, DOI didn't have any significant effect on the amplitude of eEPSP elicited by stimulation of L5p somata or the forceps minor (Tanaka & North, 1993).

In mouse cortical slices treated with picrotoxin (a $GABA_A$ antagonist) to isolate excitatory input, DOI (10 μM) increased the frequency of spontaneous EPSPs (sEPSP) in L5p cells two- to tenfold (mean 350%) after 6–10 minutes of treatment, and the effect did not desensitize over a 20-minute application. LY379268 reversed sEPSP below control levels (Kłodzinska et al., 2002).

DOB elicited a time and concentration -dependent modulation of EPSPs that matched that of EPSCs (Arvanov et al., 1999a). At 1 μM, DOB increased eEPSP amplitude evoked by forceps minor's stimulation in most L5/6p neurons. This facilitatory effect was lost after 5–15 minutes, followed by an inhibitory effect (Arvanov et al., 1999a). At 20 μM, DOB reduced the amplitude of eEPSP in all cells, and this inhibitory effect is potentiated after 20 minutes, during which the RMP is slowly depolarized (Arvanov et al., 1999a).

DOI (3 μM, 10-15 min) induced the appearance of late eEPSP following rhythmic (0.1 Hz) stimulation of forceps minor fibers (Marek & Ramos, 2018). Late eEPSP were larger in amplitude than early eEPSP (9.8 mV vs 5.3 mV) and were preferentially and dose-dependently suppressed by β_2 activation (Marek & Ramos, 2018).

3.1.3. Action Potentials

3.1.3.1 Intrinsic excitability

The reports of psychedelic action on neural intrinsic excitability are inconsistent. Early research in rat mPFC slices reported that DOI markedly increases the number of spikes

elicited by a depolarizing current pulse in L5p neurons. This effect has a slow onset and is antagonized by ketanserin (Araneda & Andrade, 1991). However, subsequent experiments found that DOI elicits only a slight, non-significant increase in the number of spikes (Lambe & Aghajanian, 2006).

In mouse mPFC slices, it has been recently shown that NBOH elicits a significant, dose-dependent decrease in total spike output from L5p neurons during a current injection (Ekins et al., 2023; Wang et al., 2025). This is accompanied by significant decreases in average firing frequency, maximum firing frequency, and firing frequency-current input gain (Ekins et al., 2023). Similar inhibitory effects were reported for DOI and 4-OH-DiPT. The loss in frequency-current gain was more pronounced when NBOH was bath-applied compared to intracellular delivery, suggesting that the action is mediated by extracellular 5-HT_{2A} (Ekins et al., 2023).

The firing frequency after combining NBOH (0.1 or 10 μM) with 5-HT_{2A} antagonists was significantly lower than with antagonists alone, suggesting that 5-HT_{2A} does not mediate the inhibitory effect at these concentrations (Ekins et al., 2023; Wang et al., 2025). In turn, XE-991 blocked the decreased firing by 1 or 10 μM NBOH, but failed to do so for 100 μM NBOH, indicating that K_v7 channels are involved in the inhibitory action of NBOH at concentrations of 1–10 μM, but not of 100 μM (Ekins et al., 2023; Wang et al., 2025).

However, the findings of Ekins et al. (2023) and Wang et al. (2025) should be interpreted with caution. We have already noted the use of concentrations high above drug affinity for 5-HT_{2A}. Additionally, pharmacological tests with 5-HT_{2A} antagonists (ketanserin or M100907) and XE-991 lack within-cell comparisons across baseline, drug, antagonist, and combined conditions, limiting causal interpretation. The absence of these controls is particularly critical given the high inter-cellular variability observed in drug responses (Ekins et al., 2023; Wang et al., 2025). Moreover, the ability of 10 μM ketanserin to effectively block 10 μM NBOH is questionable, as 2.2 nM NBOH inhibits 50% of 0.5 nM ketanserin binding to 5-HT_{2A} (Halberstadt et al., 2016).

3.1.3.2 Burst Firing

DOB (0.1 μM) increased burst firing frequency elicited by NMDA by 448%. Bicuculline does not prevent the increase, suggesting that it is not due to interneuron disinhibition. By contrast, 20 μM DOB decreased bursting frequency to 17% in the same cells that were excited by 0.1 μM DOB (Arvanov et al., 1999a).

In mouse mPFC slices treated with $GABA_A$ and AMPAR/KAR antagonists to isolate L5p neurons from both inhibitory and excitatory inputs, TCB-2 elicited recurrent oscillatory bursts (ROBs) after 15–20 s of tonic spiking induced by a depolarizing current, in 50% of the cells tested. Neurons that exhibited ROBs had significantly larger depolarizing sags in response to hyperpolarizing currents. ROBs were observed when neurons are held at just suprathreshold potentials, with the maximum effect at 116% of rheobase. They were blocked by ketanserin and disappeared after 5–10 min of washout (Spindle & Thomas, 2014).

ROBs did not appear in the absence of GABAR and AMPAR/KAR antagonists. In the absence of $GABA_A$ antagonists, large inhibitory postsynaptic potentials (IPSPs), down to -10 mV, appeared to bias neurons toward tonic spiking when entering the ROB mode. Similar ROB discharges have been reported following the focal application of glutamate to the apical dendrites of L5p or could be elicited by concurrent stimulation of the apical dendrites and soma of L5p (Spindle & Thomas, 2014).

3.1.3.3 Spontaneous Firing Frequency

Focal application of psilocin to untagged L5p neurons within cortical slices increased the firing frequency in 53% of cells, while 26% were inhibited and the rest remained unchanged. In this experiment, excitation and inhibition were defined as ±20% changes from the baseline firing frequency. By contrast, in L5p neurons tagged with a $5\text{-}HT_{2A}$-GFP fusion protein, psilocin or NBOH increased the firing frequency by 200% in all cells (Schmitz et al., 2022).

When $5\text{-}HT_{2C}$ receptors were antagonized, the basal firing frequency decreased. Subsequent application of psilocin or NBOH reversed the decrease and raised the firing frequency by 200%. Focal application of either a $5\text{-}HT_{2A}$ antagonist or a $G\alpha_{q/11}$ inhibitor also reduced basal firing frequency, but this decrease could be reversed by psilocin or NBOH (Schmitz et al., 2022).

The intracellular delivery of the $G\alpha_{q/11}$ inhibitor made psilocin reduce the firing frequency of L5p neurons, which was not observed with NBOH. The discrepancy can be explained by the fact that psilocin can still recruit $G\alpha_{i/o}$ signaling via $5\text{-}HT_{1A}$ receptors in the presence of $G\alpha_{q/11}$ inhibitors, while NBOH is selective for $G\alpha_{q/11}$-coupled 5-HT receptors (Schmitz et al., 2022).

3.1.3.4 Spike Frequency Adaptation, Afterhyperpolarization and Spike Amplitude

Several studies report that DOB decreases spike frequency adaptation in trains of action potentials elicited by a depolarizing pulse in rat mPFC slices (Araneda & Andrade, 1991; Arvanov et al., 1999a). This effect could be prevented by TTX plus bicuculline (Arvanov et al., 1999a).

The findings from the preprint by Ekins et al. (2023) conflict with these results, showing a significant, concentration-dependent increase in frequency adaptation after NBOH treatment in mouse mPFC slices. The adaptation index was not significantly different after combining XE-991 with NBOH, compared to XE-991 alone, suggesting that blocking K_V7 channels occludes frequency adaptation. However, these pharmacological manipulations lack a comparison with NBOH treatment alone and vehicle controls.

Spike afterhyperpolarization (AHP) is mediated by the opening of K^+ channels and is closely linked to frequency adaptation. DOI or DOB decreased AHP in L5p neurons from rat mPFC slices (Araneda and Andrade, 1991; Arvanov et al., 1999a; Villalobos et al., 2005), with one study reporting the replacement of AHP by a slow depolarizing afterpotential following a train of spikes (Araneda & Andrade, 1991). AHP can be decomposed in an early and a slowly-decaying component. DOB reduced the latter along with the current that mediates it, an action that could be blocked by 5-HT_{2A} antagonism (Arvanov et al., 1999a; Villalobos et al., 2005).

Spike amplitude modulation has been inconsistently reported. Some studies in rat cortical slices report non-significant increases or decreases after DOI or DOB treatments (Arvanov et al., 1999a; Lambe & Aghajanian, 2006). In mouse cortical slices, Ekins et al. (2023) report a significant, concentration-dependent decrease in spike amplitude (-2% to -19%) following 0.1–100 μM NBOH. Similarly, 4-OH-DiPT at 10 μM caused a 2% decrease in spike amplitude, while 100 μM caused a 12% decrease. In turn, DOI showed an 8% decrease in spike amplitude at 10 μM but only a 4% decrease at 100 μM.

3.2 In Vivo Studies

Results of *in vivo* studies are compiled in Table 2.

3.2.1 Local Application

Microiontophoretic DOI delivery to the frontal cortex of rats, mice, and guinea pigs consistently induces current-dependent inhibition of both spontaneous and quisqualate (an AMPAR agonist) -induced firing in L5/6p neurons from animals anesthetized with chloral hydrate (Ashby et al., 1989; Ashby & Wang, 1990; Bambico et al., 2010; Bergqvist et al., 1999; El Mansari & Blier, 1997, 2005; Rueter & Blier, 1999; Reuter et al., 2000). However,

at lower ejecting currents (0.5 nA), DOI exerted a facilitatory effect on glutamate-induced firing in the mPFC, increasing firing rates in a fraction of the cells tested, whereas higher currents (>10 nA) suppressed all cells (Ashby et al., 1989; Ashby et al., 1994). Ritanserin and 5-HT_{1A} activation prevented the excitatory effect at low ejecting currents (Ashby et al., 1994). This biphasic modulation aligns with *in vitro* results from Arvanov et al. (1999a).

In the mPFC, DOI's inhibitory action was unaffected by $MgCl_2$ (which prevents neurotransmitter release) but was blocked by several atypical neuroleptics, such as clozapine, ritanserin or risperidone, suggesting a direct, 5-HT_{2A}-mediated mechanism (Ashby et al., 1989; Ashby and Wang, 1990; Bergqvist et al., 1999; Reuter and Blier, 1999). In contrast, in the OFC, DOI's inhibition remained unaffected by atypical neuroleptics (Bergqvist et al., 1999; El Mansari and Blier, 1997), and by bicuculline (a $GABA_A$ antagonist) (Bergqvist et al., 1999), but was blocked by the selective 5-HT_{2A} antagonist M100907 (Reuter et al., 2000). Intriguingly, knocking out 5-HT_{2C} receptor did not affect DOI's inhibitory effect in the OFC, but abolished M100907's blocking action (Reuter et al., 2000).

In mice, knocking out the fatty acid amide hydrolase (FAAH) significantly reduced DOI's inhibitory effects, suggesting endocannabinoids play a modulatory role (Bambico et al., 2010).

However, one study presented conflicting results in mice, reporting a current-dependent increase in the firing rates of L5p following DOI application (20–50 nA) (De Gregorio et al., 2021). The discrepancy may stem from methodological differences: the use of urethane anesthesia, rather than chloral hydrate, and the use of NMDA to activate neurons within their physiological firing rates, rather than quisqualate. The excitatory response to local DOI administration was further enhanced after chronic systemic LSD treatment, an effect significantly attenuated by Raptor KO (De Gregorio et al., 2021). Raptor, an adaptor protein involved in mTORC1 signaling, is linked to neural plasticity, suggesting that chronic LSD effects may involve mTOR-dependent synaptogenesis (Ly et al., 2018).

Local DOI delivery into the mPFC by microdialysis significantly increased 5-HT release. This effect can be potentiated by DAMGO (a μ-opioid receptor agonist) and LY-379268 (a mGlu II receptor agonist) (Puig et al., 2003), raising the question of how endogenous 5-HT receptor activation contributes to DOI's effects.

3.2.2 Systemic Administration in Anesthetized Animals

3.2.2.1 Firing activity

In chloral hydrate-anesthetized rats, systemic DOI administration produced a two-fold increase in the average firing rate of mPFC L5p neurons projecting either to the dorsal raphe or ventral tegmental area. About 40% of these neurons showed nearly quintupled firing rates, while 30% displayed a tenfold reduction from baseline activity. At the single neuron level, firing rate increases can reach up to 1525%, with the lower average rate attributed to the low baseline firing rates of some neurons. No significant differences in baseline firing rates could be observed between projecting L5p neurons that are upregulated, downregulated, or unaffected by DOI (Puig et al., 2003).

In neurons upregulated by DOI, burst firing increased concurrently, whereas in those where firing was downregulated, burst firing decreased (Celada et al., 2008). In most excited neurons, the firing rate increase was abolished by M100907 and LY-379268. In inhibited neurons, M100907 reversed the firing rate decrease in all cases. These findings suggest that the increase in firing rates is primarily mediated by 5-HT_{2A} agonism and glutamate release, yet 5-HT_{2A} activation also leads to neuronal inhibition in a subset of L5p neurons. Notably, M100907 remained effective in rats with thalamic lesions, indicating that firing rate modulation is mediated by non-thalamic 5-HT_{2A} receptors (Puig et al., 2003). The $GABA_A$ antagonist picrotoxin also reversed systemic DOI's inhibitory effects in the rat mPFC (Puig et al., 2003), contrasting with Bergqvist et al. (1999), who observed no reversal of local DOI's inhibition by bicuculline in the rat OFC.

A combination of 5-MeO-DMT and the monoamine oxidase inhibitor (MAOI) clorgyline—loosely mimicking ayahuasca—produced similar effects: firing rates increased in half of the L5p neurons by an average of 406%, while 35% of neurons decreased their firing to 31% of baseline, resulting in an average net increase of 215% (Riga et al., 2014). Burst firing also increased. Both clozapine and haloperidol reversed the effects on firing rates and bursting (Riga et al., 2014).

While DOI does not activate 5-HT_{1A} receptor, that has inhibitory effects on L5p neurons (Nichols, 2016), 5-MeO-DMT stands out among psychedelics due to its higher affinity for 5-HT_{1A} than for 5-HT_{2A} (Puigseslloses et al., 2024). Therefore, it is surprising that DOI reduced L5p firing to a greater extent than 5-MeO-DMT (tenfold vs. two thirds decrease), and that almost the same proportion of cells was inhibited (30% vs. 35%) (Puig et al., 2003; Riga et al., 2014). These findings further support that 5-HT_{2A} is involved in the inhibitory action of psychedelics.

An acute dose of LSD had no significant effect on firing rates. Chronic LSD administration increased bursting activity in L5p neurons, yet it did not increase firing rates. Additionally,

chronic LSD potentiated the excitatory response to quisqualate, but not to NMDA, nor the inhibitory action of the 5-HT_{1A} agonist 8-OH-DPAT. As noted earlier, the effects of chronic LSD are attenuated by Raptor KO and may be attributed to dendritic and synaptic plasticity (De Gregorio et al., 2021).

Despite the increase in firing rates elicited by 5-MeO-DMT, the BOLD signal in the mPFC and the primary visual cortex (V1) was significantly reduced. This discrepancy between electrophysiological and fMRI recordings could not be explained by alterations in blood pO_2 or pCO_2 (Riga et al., 2014). Additional studies have observed decreased BOLD signals in rats and humans following psychedelic administration (Carhart-Harris et al., 2012; Ghaw et al., 2024). Although firing rates are increased in L5p projecting neurons (Puig et al., 2003; Riga et al., 2014; Shao et al., 2025), psychedelics exert an overall inhibitory effect on neuronal firing (Brys et al., 2023; Dearnley et al., 2021). Another possible explanation for this discrepancy is that psychedelics may reduce aerobic metabolism, as suggested by the downregulation of mitochondrial genes and induction of resistance to hypoxia and ischemia in tissues (Nardai et al., 2020; Szabo et al., 2016; Szabó et al., 2021; Zhou et al., 2025).

Under ketamine anesthesia, LSD (30-60 µg/kg, i.p.) did not change PFC firing rates (Godbout et al., 1991). Moreover, it markedly prolonged the inhibition of PFC neurons following electrical stimulation of the ventral tegmental area, which could be prevented using a 5-HT_{2A} antagonist (Godbout et al., 1991). Congruent with this finding, under urethane anesthesia, LSD could increased mPFC firing frequency only at the highest dose tested (160 µg/kg, i.p.) (Inserra et al., 2021). No significant change in burst firing was observed. By contrast, at lower doses (10–80 µg/kg, i.p.), all tested neurons in the mediodorsal nucleus (MD) of the thalamus increased both their firing frequency and bursting, while in the reticular nucleus, half of the neurons were excited and the other half inhibited. Haloperidol was able to rescue the inhibition in the reticular nucleus (Inserra et al., 2021).

3.2.2.2 Local Field Potentials

Both DOI and 5-MeO-DMT reduced low-frequency oscillations (LFO, <4 Hz) within mPFC local field potentials (LFP), with 5-MeO-DMT additionally suppressing LFO in V1 and other unimodal cortices (Celada et al., 2008; Riga et al., 2014, 2016). This suppression occurred independently of whether the firing rate of a recorded neuron was increased or decreased (Riga et al., 2014). Notably, the proportion of spikes occurring during the active phase of LFO, defined as the portion below its mean voltage value, decreased indicating a

decoupling of oscillatory activity from spike timing (Celada et al., 2008). The LFO reduction was partially or completely blocked by 5-HT_{2A} antagonists, atypical neuroleptics and 5-HT_{2A} KO (Celada et al., 2008; Riga et al., 2014, 2016). For 5-MeO-DMT specifically, the 5-HT_{1A} antagonist WAY-100635 and the mGlu II agonist LY-379268 also blocked LFO suppression (Riga et al., 2014, 2016).

3.2.3 Systemic Administration in Awake Animals

3.2.3.1 Firing activity

Awake animal studies mostly report inhibitory or neutral effects of psychedelics on neuronal firing (Brys et al., 2023; Dearnley et al., 2021; Gener et al., 2019; Wood et al., 2012).

The most comprehensive electrophysiological study to date has recorded 3,612 mPFC neurons in mice following TCB-2 administration, a highly 5-HT_{2A}-selective psychedelic (Dearnley et al., 2021). [For a peer-reviewed version of this work, but focusing on the comparison of TCB-2's effects to arousal, see (Dearnley et al., 2023). For the complete PhD thesis, see (Dearnley, 2023)]. However, this study did not isolate L5p neurons from other neural types. Of all neurons, 11% were significantly excited, and 21% were inhibited. Although the mean logarithmic firing rate decreased significantly, the average firing rate and the total number of spikes remained stable, due to a redistribution in spiking activity. The distribution of decreased logarithmic rates shifted leftward and became more dispersed, while that of increased log-rates became more condensed to the right (Dearnley et al., 2021). This pattern, where inhibition of many neurons offsets excitation of fewer fast-spiking (typically non-pyramidal) cells, challenges the simplistic view of psychedelics as uniformly excitatory in the mPFC, which is at the basis of some of the leading hypotheses about psychedelic action.

These compensatory dynamics may be masked by firing rate normalization. Normalized firing rates of excitatory and inhibitory cells were significantly decreased by DOI and LSD in many cortical and subcortical regions of freely moving rats, including the mPFC L5p neurons, with the most significant reductions occurring in the temporal association area (Brys et al., 2023 Wood et al., 2012).

However, 16% of mouse mPFC L5p neurons projecting to the pons substantially increased their spiking activity after psilocybin injection, while only 2% are substantially inhibited, with the average firing rate being increased (Shao et al., 2025). In contrast, only 3% of L5p neurons projecting to the caudate putamen (i.e., intratelencephalic neurons) were excited,

and none were inhibited. Congruently, *in vivo* calcium imaging revealed significant increases in calcium transients in projecting, but not intratelencephalic neurons (Shao et al., 2025).

The finding that psychedelics increase the average firing rate of L5p projecting neurons is in line with the findings of Puig et al. (2003) and Riga et al. (2014) in anesthetized animals. Nevertheless, Shao et al. (2025) may have underestimated the proportion of inhibited neurons. They apply a criterion of $|Z| > 2$ to classify substantial increases or decreases in firing rates. As described by Dearnley et al. (2021), the distribution of excited neurons is concentrated toward the right, while the distribution of inhibited neurons is spread toward the left. Consequently, Shao et al. (2025) should have observed a much higher number of excited neurons in the right tail ($Z>2$) than in the left tail ($Z<-2$) of the distribution curve.

As for population-level firing, a modest decrease in multi-unit activity was seen in the mouse prelimbic frontal cortex following DOI administration (Gener et al., 2019).

3.2.3.2 Local Field Potentials

LSD and DOI increased the power and prevalence of high-frequency oscillations (HFOs) in the 100–150 Hz range within LFP recorded from the rat mPFC and other brain regions (Brys et al., 2023). The increase was significantly greater when the animals are at rest (Hansen et al., 2019). The synchronized HFOs activity across the mPFC, OFC, and ventral striatum exhibited near-zero phase lags. Granger causality analyses indicated the ventral striatum exerts the strongest influence on the mPFC (Brys et al., 2023). At lower frequency bands, 5-MeO-DMT increases mPFC-V1 coherence in the beta band (10-30 Hz), mPFC-MD coherence in the theta (4-10 Hz) and beta bands, and V1-MD coherence in the beta band (Riga et al., 2018).

The effects on gamma frequency oscillations show more variability across studies. DOI administration decreases both low (30–55 Hz) and high (55–80 Hz) gamma power in rat OFC, with the high gamma reduction diminishing at higher doses (Wood et al., 2012). In the ACC, DOI reduces both gamma sub-bands at increasing doses (Wood et al., 2012). Other studies report more modest effects in rats, with non-significant decreases in mPFC low gamma power that extend to the high gamma band when animals are at rest (Hansen et al., 2019). In turn, psilocin increases high gamma power (>60 Hz) in the mPFC and ACC in sleep-deprived mice (Thomas et al., 2022), while DOI increases mPFC high gamma power (50–100 Hz) in undisturbed mice, enhancing synchronicity between the mPFC and hippocampus, effects that are reversed by antagonizing 5-HT_{2A} (Gener et al.,

2019). As for, 5-MeO-DMT, it increases gamma power (30–80 Hz) in the mPFC via both 5-HT_{2A} and 5-HT_{1A} activation (Riga et al., 2018).

In lower-frequency bands, DOI decreases theta power (4–10 Hz) in the mPFC of resting mice (Hansen et al., 2019). In contrast, a psilocin injection given at the typical sleep onset time enhanced peak at 4 Hz only when animals were allowed to rest (Thomas et al., 2022). As for 5-MeO-DMT, i.p. injection led to a dose-dependent increase in delta (1–4 Hz) and theta (5–12 Hz) power, while intracerebroventricular (ICV) injection led to a dose-dependent decrease in theta power (Souza et al., 2024).

The correlations between oscillatory activity and spike output also show inconsistent alterations. DOI reduces the correlation between gamma oscillations and spike timing in the rat OFC and ACC (Wood et al., 2012). This result aligns with the findings of Celada et al. (2008) in mPFC LFO of anesthetized rats. However, LSD and DOI exerted a modest increase in the entrainment strength of spikes by HFOs in the rat mPFC, and increased the proportion of neurons exhibiting entrainment. The ventral striatum, which appears to drive HFO synchronicity between regions, shows particularly strong HFO-spike entrainment (Brys et al., 2023).

At the network level, LSD reduces broadband LFP power across multiple regions, including OFC and mPFC, suggesting a shift toward reduced firing (Nasretdinov et al., 2023), which is consistent with findings from Brys et al. (2023) and Dearnley et al. (2021). Furthermore, changes in LFP spectral slopes suggested an E/I balance shift toward excitation in local PFC circuits, thus, a decoupling between the network’s E/I state and spike output (Nasretdinov et al., 2023). In the temporal association area, however, there is a congruent E/I shift towards inhibition, decrease in firing activity, high HFO entrainment strength and low HFO prevalence (Brys et al., 2023; Nasretdinov et al., 2023).

As a final note, some studies have reported the emergence of sleep-like electrophysiological features in awake animals (Souza et al., 2024; Thomas et al., 2022).

4. Discussion

The aim of this review work was to facilitate a comprehensive view of electrophysiological data about the action of psychedelic drugs. This was needed in order to complement data from neuroimaging studies with more precise physiological experimentation. Our main interest was to challenge one prevailing assumption in psychedelic science: that psychedelics increase neuronal excitability in L5p neurons. We focused on the frontal cortex since it is the brain region which has been most studied, and reviewed data from *in vitro* experimentation, which afford a precise control of the recordings, as well as from *in vivo* assays that reproduce the complexity of a living brain.

4.1 Summary

Psychedelics exert a complex modulatory influence on L5p neurons, combining excitatory and inhibitory effects.

In vitro, they induce a mild but consistent depolarization of the RMP (Araneda & Andrade, 1991; Arvanov et al., 1999a; Ekins et al., 2023; Lambe & Aghajanian, 2006; Spindle & Thomas, 2014; Tanaka & North, 1993) while suppressing NMDA-evoked EPSCs/EPSPs (Arvanov et al., 1999a, 1999b). They also trigger AMPAR internalization, further dampening excitatory transmission (Berthoux et al., 2019), though a subset of L5p neurons exhibit potentiated AMPA-induced currents (Arvanov et al., 1999a). Despite these suppressive effects, psychedelics shift the E/I balance toward excitation, producing late, prolonged eEPSC/eEPSP that correspond to up states (Aghajanian & Marek, 1999; Marek & Ramos, 2018; Lambe & Aghajanian, 2006, 2007; Stutzmann et al., 2001).

Firing responses vary: some studies report marked increases in evoked and spontaneous L5p activity (Araneda & Andrade, 1991; Schmitz et al., 2022), while others observe concentration-dependent suppression (Ekins et al., 2023; Wang et al., 2025) or non-significant changes (Lambe & Aghajanian, 2006). Similarly, spike frequency adaptation may decrease (Araneda & Andrade, 1991; Arvanov et al., 1999a) or increase (Ekins et al., 2023). Notably, psychedelics consistently reduce AHP (Araneda & Andrade, 1991; Arvanov et al., 1999a; Villalobos et al., 2005).

In vivo, microiontophoretic application of DOI inhibits L5p firing (Ashby et al., 1989; Ashby & Wang, 1990; Bambico et al., 2010; Bergqvist et al., 1999; El Mansari & Blier, 1997, 2005; Reuter & Blier, 1999), whereas systemic administration yields mixed excitatory, inhibitory, or neutral effects across populations (Celada et al., 2008; Godbout et al., 1991; Inserra et al., 2021; Puig et al., 2003; Riga et al., 2014; Shao et al., 2025). The dominant

outcome is net inhibition of L5p cells (Wood et al., 2012), as well as of excitatory and inhibitory neurons more generally (Brys et al., 2023). However, this suppression is offset by increased firing in a subset of fast-spiking neurons, preserving overall mPFC spike output (Dearnley et al., 2021). See also Béïque et al. (2007); Martin & Nichols (2016)

LFP effects are inconsistent. However, most studies report reduced power in low-gamma and lower frequencies (Celada et al., 2008; Hansen et al., 2019; Riga et al., 2014, 2016; Souza et al., 2024) but elevated high-gamma and higher-frequency activity (Brys et al., 2023; Gener et al., 2019; Riga et al., 2018; Thomas et al., 2022). Some LFPs also show enhanced cross-regional synchrony (Brys et al., 2023; Gener et al., 2019; Riga et al., 2018). While LFP-spike coupling typically weakens in low-frequency and gamma bands (Celada et al., 2008; Wood et al., 2012), some report stronger HFO-spike entrainment (Brys et al., 2023).

24 hours post-administration, studies note increased mEPSC, sEPSC, and burst firing (De Gregorio et al., 2021; Ly et al., 2018; Shao et al., 2021), likely reflecting synaptic and dendritic plasticity rather than direct electrophysiological modulation.

4.2 Differential Dendritic Modulation by Psychedelics

Psychedelics appear to modulate distinct compartments of L5p neurons in a layer-specific manner. Studies stimulating L1 report increased eEPSP/eEPSC (Aghajanian & Marek, 1997; Barre et al., 2016), whereas those stimulating L5 or the forceps minor observe either unchanged eEPSP or reduced eEPSC/eEPSP (Arvanov et al., 1999a, 1999b; Tanaka & North, 1993). Additionally, stimulation of L2/3, L5 or the forceps minor at specific frequencies induces up states (Aghajanian & Marek, 1999; Lambe & Aghajanian, 2006, 2007; Stutzmann et al., 2001).

Anatomically, L1 contains thalamic fibers projecting to the apical dendritic tufts of L5p neurons, while the forceps minor innervates basal L5p dendrites. L2/3 is traversed by the apical dendritic trunks of L5p cells, and the most superficial part of L5 (L5a) contains oblique dendrites (Squire et al., 2012). Functionally, L5p neurons can be divided into three compartments: (1) a basal compartment (soma-proximal dendrites), (2) an apical compartment (tuft dendrites), and (3) a coupling compartment (apical trunk and oblique dendrites) (Aru et al., 2020; Suzuki & Larkum, 2020).

According to Dendritic Integration Theory (Bachmann et al., 2020), the basal compartment receives feedforward sensory input, whereas the apical compartment integrates cortico-cortical contextual signals. These streams converge in the coupling compartment, which is

modulated by higher-order thalamic nuclei (Aru et al., 2020; Bachmann et al., 2020). During wakefulness, apical and basal compartments remain coupled, enabling sensory-context integration. Under general anesthesia, this coupling is disrupted, isolating the two streams (Aru et al., 2020; Suzuki & Larkum, 2020). Intriguingly, the coupling region of L5p neurons concentrates the highest expression of 5HT2A proteins in the neocortex (Chiu et al., 2023; Weber & Andrade, 2010).

Psychedelics enhance EPSPs/EPSCs in the apical compartment (Aghajanian & Marek, 1997; Barre et al., 2016) while suppressing basal compartment activity (Arvanov et al., 1999a). This effect is stronger with 5-HT_{1A} agonists like LSD or 5-HT itself (Arvanov et al., 1999b; Tanaka & North, 1993), due to the receptor's dense expression in the basal compartment and axon hillock (Czyrak et al., 2003). Furthermore, psychedelics promote up states during rhythmic stimulation of the coupling compartment (Lambe & Aghajanian, 2006, 2007). Increasing the excitability of the coupling compartment is opposite to the effect of general anesthetics (Suzuki & Larkum, 2020). Indeed, recent work shows that DOI reverses propofol/isoflurane effects (Huels et al., 2025).

This shift—apical/coupling hyperexcitability combined with basal hypoexcitability—amplifies apical influence over L5p output, termed apical drive (Phillips et al., 2025). Thus, the psychedelic state may reflect contextual, top-down cortico-cortical dominance over L5p activity. Some hypotheses attribute hallucinations to increased top-down processing (Corlett et al., 2019), aligning with psychedelics reducing sensory-evoked visual cortex activity (Heiss et al., 1973; Michaiel et al., 2019). Notably, these electrophysiological findings challenge hypotheses proposing either weakened top-down constraints (Carhart-Harris & Friston, 2019) or bottom-up sensory dominance (Vollenweider & Preller, 2020).

4.3 Molecular Mechanisms of Synaptic Modulation

Most *in vitro* studies have employed "low" concentrations (<3 μM) of DOB or DOI. However, the peak forebrain concentration of DOI following a systemic dose of 1 mg/kg—a standard dose used in in vivo electrophysiological studies (Table S2)—reaches approximately 500 ng/g wet tissue weight, equivalent to ~1.5 nM (De La Fuente Revenga et al., 2019). Phenylethylamines are particularly useful for isolating the core effects of psychedelics due to their higher selectivity for 5-HT_{2A} receptors compared to tryptamines and ergolines (Nichols, 2016). At these low concentrations, 5-HT_{2A}-mediated effects follow a consistent temporal profile. Initially, DOB and DOI enhance eEPSP/eEPSC amplitudes by promoting presynaptic glutamate release (Arvanov et al., 1999a; Barre et al., 2016). However, this potentiation undergoes significant desensitization within 15–20 minutes

(Arvanov et al., 1999a). During this window, postsynaptic processes come into play. PKC drives AMPAR internalization (Berthoux et al., 2019), while CaM-KII suppresses NMDA-evoked currents (Arvanov et al., 1999a). Notably, in apical dendrites, PKC activity counters this inhibition by potentiating GluN2B-NMDAR (Barre et al., 2016), which may explain the sustained elevation of eEPSP beyond the 20-minute mark (Aghajanian and Marek, 1997). In parallel, extrasynaptic GluN2B-NMDAR-dependent up states begin to emerge (Aghajanian & Marek, 1999; Lambe & Aghajanian, 2006, 2007; Stutzmann et al., 2001). Once established, these effects can persist for hours after washout (Arvanov et al., 1999a; Berthoux et al., 2019; Lambe & Aghajanian, 2006). To provide a schematic, integrated view of these dynamics, we developed Figures 2, 3 and 4.

The early excitatory phase is absent in LSD, due to its 5-HT_{1A} activity, and is also abolished at higher concentrations of DOB (Arvanov et al., 1999a, 1999b). This concentration and time -dependence in drugs lacking 5-HT_{1A} agonism may reflect pharmacodynamic properties that favor presynaptic 5-HT_{2A} signaling at lower doses, like higher receptor affinity or reduced occupancy. Another explanation involves compartmentalized receptor signaling: presynaptic glutamate release may involve extracellular 5-HT_{2A} receptors, while postsynaptic inhibition may require intracellular receptor activation. At low concentrations, psychedelics could gradually diffuse across the membrane, activating intracellular receptors over time (Figures 3 and 4). This hypothesis also accounts for the prolonged effects observed after washout. Supporting this, the head twitch response—a rodent behavioral proxy for hallucinogenic activity—requires intracellular receptor activation. Nevertheless, extracellular receptors appear to mediate the inhibition of action potentials, as suggested by Ekins et al. (2023), although these findings should be interpreted with caution (see Section 2.3.1). However, both reports are not mutually exclusive: it is possible that postsynaptic activity is modulated by intracellular receptors while action potentials are controlled by outer plasma membrane 5-HT_{2A}. Notably, this would imply that postsynaptic activity, and not neuronal firing, is key to head twitch response.

The interplay between CaM-KII and PKC is especially intriguing. CaM-KII is a sophisticated enzyme involved in synaptic plasticity, performing key roles in both long-term potentiation (LTP) and long-term depression (LTD) (for a review, see Bayer & Giese, 2025). High levels of Ca^{2+}/calmodulin promote CaM-KII binding to GluN2B-NMDARs, facilitating LTP, whereas dissociation is linked to LTD (Bayer & Giese, 2025). Interestingly, Arvanov et al. (1999a) showed that inhibiting either CaM-KII or Ca^{2+}/calmodulin prevents

DOB-induced suppression of NMDA-evoked currents. Additionally, Barre et al. (2016) showed that PKC enhances NMDAR conductance by phosphorylating Ser1303 in GluN2B, preventing desensitization. However, this modification also disrupts CaM-KII binding (O'Leary et al., 2011). Moreover, DOI promotes internalization of GluA2-containing AMPARs through PKC, a process typically associated with LTD (Berthoux et al., 2019). Thus, suppression of LTP-related mechanisms appears to underlie desensitization to excitatory input, while LTD-associated pathways in apical dendrites maintain excitability. Adding to this paradox, rather than the spine shrinkage typically associated with LTD (Woolfrey et al., 2018), an increase in apical spine density is observed following psychedelic exposure (Shao et al., 2025). These contradictory interactions need further investigation into the roles of PKC and CaM-KII in psychedelic-induced modulation of synaptic plasticity and electrophysiology.

The modulation of GluN2B-NMDARs is remarkable in the context of psychedelic action. This subunit is unique in its sensitivity to CaM-KII (Bayer & Giese, 2025) and has been implicated in both enhanced glutamate release (Barre et al., 2016) and the generation of late eEPSC when activated at extrasynaptic sites (Lambe & Aghajanian, 2006). These processes are tightly coupled, as glutamate spillover from increased presynaptic release can activate these extrasynaptic receptors (Lambe & Aghajanian, 2006). The combined activity of presynaptic and extrasynaptic GluN2B-NMDARs likely contributes to the induction of persistent up states (Figure 4). Moreover, GluN2B-containing receptors generate low-amplitude, slow-decay currents (Vicini et al., 1998), making them well-suited for sustaining prolonged, late eEPSC (Lambe & Aghajanian, 2006). Additionally, their high mobility within the membrane allows them to redistribute from synaptic to extrasynaptic regions (Groc et al., 2006). Therefore, CaM-KII-dependent inhibition at postsynaptic sites may be followed by a receptor's reorganization that enhances extrasynaptic excitability (Figure 4). This specific regulation of GluN2B-NMDARs appears central to the sustained effects of psychedelics (see also Davoudian et al., 2023) and warrants further study.

4.4 Excitatory vs Inhibitory Action of Psychedelics

In vitro studies show that L5p neurons highly expressing 5-HT_{2A} consistently increase their firing rates (Schmitz et al., 2022). *In vivo*, psychedelics increase the average firing of L5p neurons projecting to brainstem regions (Celada et al., 2008; Puig et al., 2003; Riga et al., 2014; Shao et al., 2025). These types of L5p cells are type I neurons (Elliott et al., 2018). Type I neurons are fewer in number, project outside the telencephalon to structures like the brainstem or the thalamus, have prominent and complex apical compartments, and

respond to 5-HT with a strong 5-HT_{2A}-mediated excitatory current. In contrast, type II neurons are more common, project to intratelencephalic regions, have larger basal compartments, and respond to 5-HT with more modest responses, most often inhibitory currents dependent on 5-HT_{1A} activity (Elliot et al., 2018). Therefore, psychedelics seem to specifically increase the firing of a subset of 5-HT_{2A}-expressing type I neurons. These are likely the minority of cells where DOB elicited a concentration-dependent potentiation of AMPA-evoked currents (Arvanov et al., 1999a).

Consistent with the higher prevalence of type II neurons (Elliot et al., 2018), most L5p cells are inhibited by psychedelics (Wood et al., 2012). This inhibition is 5-HT_{2A}-dependent and involves GABAergic transmission (Puig et al., 2003). A minority of 5-HT_{2A}-expressing cells are parvalbumin-positive, fast-spiking interneurons (Weber & Andrade, 2010), in line with Dearnley et al. (2021) reporting a small subset of excited fast-spiking neurons offsetting the firing rates of a large number of inhibited cells.

However, DOI, lacking 5-HT_{1A} activity, consistently inhibits the firing of most L5p neurons when applied locally (Ashby et al., 1989; Ashby & Wang, 1990; Bambico et al., 2010; Bergqvist et al., 1999; El Mansari & Blier, 1997; Reuter & Blier, 1999). In contrast, it only excites a varying subset of L5p neurons when administered systemically (Celada et al., 2008; Puig et al., 2003; Riga et al., 2014; Shao et al., 2025). Moreover, upon local administration, L5p inhibition persists in the presence of picrotoxin and $MgCl_2$ (Ashby et al., 1989; Bergqvist et al., 1999), suggesting a direct, 5-$HT_{2A/C}$-mediated mechanism.

We have seen that psychedelics inhibit postsynaptic currents through 5-HT_{2A} receptors (Arvanov et al., 1999a; Berthoux et al., 2019). Another potential direct inhibitory mechanism of 5-HT_{2A} receptors involves the recruitment of pertussis toxin-sensitive $G\alpha_{i/o}$ signaling by 5-HT_{2A} receptors (González-Maeso et al., 2007; Kurrasch-Orbaugh et al., 2003). Alternatively, psychedelics may hinder firing by rapidly and selectively inducing 5-HT_{2A} internalization in L5p axons, as suggested by experiments using iPSC-derived human cortical neurons (Schmidt et al., 2024). Additionally, DOI-induced inhibition could be mediated by 5-HT_{2C} receptors, which are co-expressed with 5-HT_{2A} in L5p neurons (Nocjar et al., 2015). However, knocking out the 5-HT_{2C} receptor does not prevent DOI's inhibitory effect on L5p firing, although it intriguingly abolishes the blocking action of 5-HT_{2A} antagonism on DOI (Reuter et al., 2000). More research is needed to address this issue.

$G\alpha_{i/o}$ recruitment by 5-HT_{2A} activity is selective to psychedelic-triggered signaling, since lisuride does not engage this pathway (González-Maeso et al., 2007). Interestingly, lisuride and BL 3912A (a non-hallucinogenic DOB analog) also fail to inhibit NMDA currents, in

contrast to their hallucinogenic congeners (Arvanov et al., 1999b). Since inhibition seems to be a characteristic feature of psychedelic vs non-hallucinogenic 5-HT_{2A} agonists, the question of whether increased neural excitability truly underlies psychedelic experiences arises. For instance, optogenetic activation of neurons where DOI increases Ca^{2+} transients does not elicit the head twitch response in mice (Muir et al., 2024).

Beyond 5-HT_{2A} receptor activity, a recent K_v7-mediated mechanism of action potential inhibition has been reported (Ekins et al., 2023; Wang et al., 2025). Although these works having certain limitations regarding their pharmacological protocols (see section *Intrinsic excitability*), this novel mechanism warrants further investigation.

Our findings show that, although 5-HT_{2A} is a canonical $G\alpha_{q/11}$-coupled GPCR (Kim et al., 2020), and its activation by physiological levels of 5-HT typically produces an excitatory response (Araneda & Andrade, 1991; Arvanov et al., 1999b), psychedelics exert a generalized inhibitory effect on L5p neurons, mediated by both direct L5p modulation and GABAergic activity (Ashby et al., 1989; Bergqvist et al., 1999; Puig et al., 2003; Wood et al., 2012). Along with that inhibition, a subset of projecting L5p neurons are hyperactivated (Elliot et al., 2018; Shao et al., 2025; Schmitz et al., 2022). These neurons are in a privileged position to act like cisterns that integrate large amounts of top-down activity and send it outside the telencephalon, while those inhibited are best suited to receive bottom-up input from specific thalamic nuclei (Aru et al., 2020). Additionally, higher-order thalamocortical fibers project back to the coupling compartment of L5p neurons, producing up states that boost apical drive (Aru et al., 2020; Lambe & Aghajanian, 2006; Phillips et al., 2025). This creates a scenario where the psychedelic experience coincides with a decoupling of context-driven neurons from sensory-driven ones. This pure integrative experience fits with the feelings of understanding and revelation, often without a clear content, elicited by psychedelics in human beings (Nichols, 2016). Future research should further explore the specific implications of such functional reorganization by psychedelic drugs.

5. Conclusion

This review reveals the complexity of the electrophysiological actions of serotonergic psychedelics on L5p neurons in the PFC. Contrary to the widespread assumption that psychedelics uniformly enhance cortical excitability, the evidence shows diverse, often opposing effects depending on dose, receptor localization, and neuronal compartment. Psychedelics influence membrane potential, synaptic transmission, firing patterns, and

oscillatory dynamics. These nuanced effects cannot be fully captured by neuroimaging alone, highlighting the indispensable value of electrophysiological approaches. Furthermore, the review supports the hypothesis that psychedelics promote apical drive in L5p neurons, potentially shifting the balance of cortical processing toward top-down influence. This has significant implications for our understanding of psychedelic-induced altered states of consciousness and challenges prevailing models. Moving forward, integrative studies combining electrophysiology, imaging, and computational modeling will be essential to unravel the multi-scale mechanisms underlying psychedelic effects on brain function.

Funding Sources

This research did not receive any specific grant from funding agencies in the public, commercial, or not-for-profit sectors.

Acknowledgements

Graphical Abstract: Created in BioRender. Jiménez, J. (2025) https://BioRender.com/v78d6y0

Figure 1: Created with PRISMA flow diagram generator (Haddaway et al., 2022)

Figure 2: Created in BioRender. Jiménez, J. (2025) https://BioRender.com/8tc7nxw

Figure 3: Created in BioRender. Jiménez, J. (2025) https://BioRender.com/6xk0pkn

Figure 4: Created in BioRender. Jiménez, J. (2025) https://BioRender.com/ds00zvg

References

Aghajanian, G. K., & Marek, G. J. (1997). Serotonin Induces Excitatory Postsynaptic Potentials in Apical Dendrites of Neocortical Pyramidal Cells. *Neuropharmacology*, *36*(4–5), 589–599. https://doi.org/10.1016/S0028-3908(97)00051-8

Aghajanian, G. K., & Marek, G. J. (1999). Serotonin, via 5-HT receptors, increases EPSCs in layer V pyramidal cells of prefrontal cortex by an asynchronous mode of

glutamate release. *Brain Research*, *825*(1–2), 161–171. https://doi.org/DOI: 10.1016/s0006-8993(99)01224-x

Araneda, R., & Andrade, R. (1991). 5-Hydroxytryptamine2 and 5-Hydroxytryptamine 1A Receptors Mediate Opposing Responses On Membrane Excitability in Rat Association Cortex. *Neuroscience*, *40*(2), 399–412. https://doi.org/10.1016/0306-4522(91)90128-b

Aru, J., Suzuki, M., & Larkum, M. E. (2020). Cellular Mechanisms of Conscious Processing. *Trends in Cognitive Sciences*, *24*(10), 814–825. https://doi.org/10.1016/j.tics.2020.07.006

Arvanov, V. L., Liang, X., Magro, P., Roberts, R., & Wang, R. Y. (1999a). A pre- and postsynaptic modulatory action of 5-HT and the 5-HT2A, 2C receptor agonist DOB on NMDA-evoked responses in the rat medial prefrontal cortex. *European Journal of Neuroscience*, *11*(8), 2917–2934. https://doi.org/10.1046/j.1460-9568.1999.00708.x

Arvanov, V. L., Liang, X., Russo, A., & Wang, R. Y. (1999b). LSD and DOB: Interaction with 5-HT2A receptors to inhibit NMDA receptor-mediated transmission in the rat prefrontal cortex. *European Journal of Neuroscience*, *11*(9), 3064–3072. https://doi.org/10.1046/j.1460-9568.1999.00726.x

Ashby, C. R., Edwards, E., Harkins, K., & Wang, R. Y. (1989). Effects of (±)-DOI on medial prefrontal cortical cells: A microiontophoretic study. *Brain Research*, *498*(2), 393–396. https://doi.org/10.1016/0006-8993(89)91124-4

Ashby, C. R., Edwards, E., & Wang, R. Y. (1994). Electrophysiological evidence for a functional interaction between 5-HT1A and 5-HT2A receptors in the rat medial prefrontal cortex: An iontophoretic study. *Synapse (New York, N.Y.)*, *17*(3), 173–181. https://doi.org/10.1002/syn.890170306

Ashby, C. R., & Wang, R. Y. (1990). Effects of antipsychotic drugs on 5-HT2 receptors in the medial prefrontal cortex: Microiontophoretic studies. *Brain Research*, *506*(2), 346–348. https://doi.org/10.1016/0006-8993(90)91278-o

Bachmann, T., Suzuki, M., & Aru, J. (2020). Dendritic integration theory: A thalamo-cortical theory of state and content of consciousness. *Philosophy and the Mind Sciences*, *1*(II), Article II. https://doi.org/10.33735/phimisci.2020.ii.52

Bambico, F. R., Cassano, T., Dominguez-Lopez, S., Katz, N., Walker, C. D., Piomelli, D., & Gobbi, G. (2010). Genetic Deletion of Fatty Acid Amide Hydrolase Alters Emotional Behavior and Serotonergic Transmission in the Dorsal Raphe, Prefrontal Cortex, and Hippocampus. *Neuropsychopharmacology*, *35*(10), 2083–2100. https://doi.org/10.1038/npp.2010.80

Barre, A., Berthoux, C., De Bundel, D., Valjent, E., Bockaert, J., Marin, P., & Bécamel, C. (2016). Presynaptic serotonin 2A receptors modulate thalamocortical plasticity and associative learning. *Proceedings of the National Academy of Sciences*, *113*(10). https://doi.org/10.1073/pnas.1525586113

Bayer, K. U., & Giese, K. P. (2025). A revised view of the role of CaMKII in learning and memory. *Nature Neuroscience*, *28*(1), 24–34. https://doi.org/10.1038/s41593-024-01809-x

Béïque, J.-C., Campbell, B., Perring, P., Hamblin, M. W., Walker, P., Mladenovic, L., & Andrade, R. (2004). Serotonergic Regulation of Membrane Potential in Developing Rat Prefrontal Cortex: Coordinated Expression of 5-Hydroxytryptamine (5-HT)1A , 5-HT2A , and 5-HT7 Receptors. *The Journal of Neuroscience*, *24*(20), 4807–4817. https://doi.org/10.1523/JNEUROSCI.5113-03.2004

Béïque, J.-C., Imad, M., Mladenovic, L., Gingrich, J. A., & Andrade, R. (2007). Mechanism of the 5-hydroxytryptamine 2A receptor-mediated facilitation of synaptic activity in prefrontal cortex. *Proceedings of the National Academy of Sciences*, *104*(23), 9870–9875. https://doi.org/10.1073/pnas.0700436104

Bergqvist, P. B. F., Dong, J., & Blier, P. (1999). Effect of atypical antipsychotic drugs on 5-HT 2 receptors in the rat orbito-frontal cortex: An in vivo electrophysiological study. *Psychopharmacology*, *143*(1), 89–96. https://doi.org/10.1007/s002130050923

Berthoux, C., Barre, A., Bockaert, J., Marin, P., & Bécamel, C. (2019). Sustained Activation of Postsynaptic 5-HT2A Receptors Gates Plasticity at Prefrontal Cortex

Synapses. *Cerebral Cortex*, *29*(4), 1659–1669. https://doi.org/10.1093/cercor/bhy064

Brys, I., Barrientos, S. A., Ward, J. E., Wallander, J., Petersson, P., & Halje, P. (2023). 5-HT2AR and NMDAR psychedelics induce similar hyper-synchronous states in the rat cognitive-limbic cortex-basal ganglia system. *Communications Biology*, *6*(1), 737. https://doi.org/10.1038/s42003-023-05093-6

Carhart-Harris, R. L., Erritzoe, D., Williams, T., Stone, J. M., Reed, L. J., Colasanti, A., Tyacke, R. J., Leech, R., Malizia, A. L., Murphy, K., Hobden, P., Evans, J., Feilding, A., Wise, R. G., & Nutt, D. J. (2012). Neural correlates of the psychedelic state as determined by fMRI studies with psilocybin. *Proceedings of the National Academy of Sciences of the United States of America*, *109*(6), 2138–2143. https://doi.org/10.1073/pnas.1119598109

Carhart-Harris, R. L., & Friston, K. J. (2019). REBUS and the Anarchic Brain: Toward a Unified Model of the Brain Action of Psychedelics. *Pharmacological Reviews*, *71*(3), 316. https://doi.org/10.1124/pr.118.017160

Carhart-Harris, R. L., Leech, R., Hellyer, P. J., Shanahan, M., Feilding, A., Tagliazucchi, E., Chialvo, D. R., & Nutt, D. (2014). The entropic brain: A theory of conscious states informed by neuroimaging research with psychedelic drugs. *Frontiers in Human Neuroscience*, *8*, 20. https://doi.org/10.3389/fnhum.2014.00020

Celada, P., Puig, M. V., Díaz-Mataix, L., & Artigas, F. (2008). The Hallucinogen DOI Reduces Low-Frequency Oscillations in Rat Prefrontal Cortex: Reversal by Antipsychotic Drugs. *Biological Psychiatry*, *64*(5), 392–400. https://doi.org/10.1016/j.biopsych.2008.03.013

Chiu, Y.-T., Deutch, A. Y., Wang, W., Schmitz, G. P., Huang, K. L., Kocak, D. D., Llorach, P., Bowyer, K., Liu, B., Sciaky, N., Hua, K., Chen, C., Mott, S. E., Niehaus, J., DiBerto, J. F., English, J., Walsh, J. J., Scherrer, G., Herman, M. A., … Roth, B. L. (2023). *A suite of engineered mice for interrogating psychedelic drug actions*. bioRxiv. https://doi.org/10.1101/2023.09.25.559347

Corlett, P. R., Horga, G., Fletcher, P. C., Alderson-Day, B., Schmack, K., & Powers, A. R. (2019). Hallucinations and Strong Priors. *Trends in Cognitive Sciences*, *23*(2), 114–127. https://doi.org/10.1016/j.tics.2018.12.001

Czyrak, A., Czepiel, K., Maćkowiak, M., Chocyk, A., & Wedzony, K. (2003). Serotonin 5-HT1A receptors might control the output of cortical glutamatergic neurons in rat cingulate cortex. *Brain Research*, *989*(1), 42–51. https://doi.org/10.1016/s0006-8993(03)03352-3

Davis, A. K., Barrett, F. S., May, D. G., Cosimano, M. P., Sepeda, N. D., Johnson, M. W., Finan, P. H., & Griffiths, R. R. (2021). Effects of Psilocybin-Assisted Therapy on Major Depressive Disorder. *JAMA Psychiatry*, *78*(5), 1–9. https://doi.org/10.1001/jamapsychiatry.2020.3285

Davoudian, P. A., Shao, L.-X., & Kwan, A. C. (2023). Shared and Distinct Brain Regions Targeted for Immediate Early Gene Expression by Ketamine and Psilocybin. *ACS Chemical Neuroscience*, *14*(3), 468–480. https://doi.org/10.1021/acschemneuro.2c00637

De Gregorio, D., Popic, J., Enns, J. P., Inserra, A., Skalecka, A., Markopoulos, A., Posa, L., Lopez-Canul, M., He, Q., Lafferty, C. K., Britt, J. P., Comai, S., Aguilar-Valles, A., Sonenberg, N., & Gobbi, G. (2021). Lysergic acid diethylamide (LSD) promotes social behavior through mTORC1 in the excitatory neurotransmission. *Proceedings of the National Academy of Sciences*, *118*(5), e2020705118. https://doi.org/10.1073/pnas.2020705118

De La Fuente Revenga, M., Shin, J. M., Vohra, H. Z., Hideshima, K. S., Schneck, M., Poklis, J. L., & González-Maeso, J. (2019). Fully automated head-twitch detection system for the study of 5-HT2A receptor pharmacology in vivo. *Scientific Reports*, *9*(1), 14247. https://doi.org/10.1038/s41598-019-49913-4

Dearnley, B., Dervinis, M., Shaw, M., & Okun, M. (2021). *Stretching and squeezing of neuronal log firing rate distribution by psychedelic and intrinsic brain state transitions* (p. 2021.08.22.457198). bioRxiv. https://doi.org/10.1101/2021.08.22.457198

Dearnley, B. J. (2023). *Structure of neuronal log firing rate reorganisation in psychedelic and intrinsic brain state transitions* [Doctoral dissertation, University of Leicester]. https://figshare.le.ac.uk/articles/thesis/Structure_of_neuronal_log_firing_rate_reorganisation_in_psychedelic_and_intrinsic_brain_state_transitions/22324843

Dearnley, B., Jones, Melissa, Dervinis, Martynas, & Okun, Michael. (2023). Brain state transitions primarily impact the spontaneous rate of slow-firing neurons. *Cell Reports*, *42*(10), 113185. https://doi.org/10.1016/j.celrep.2023.113185

Deco, G., Cruzat, J., Cabral, J., Knudsen, G. M., Carhart-Harris, R. L., Whybrow, P. C., Logothetis, N. K., & Kringelbach, M. L. (2018). Whole-Brain Multimodal Neuroimaging Model Using Serotonin Receptor Maps Explains Non-linear Functional Effects of LSD. *Current Biology*, *28*(19), 3065-3074.e6. https://doi.org/10.1016/j.cub.2018.07.083

dos Santos, R. G., Bouso ,José Carlos, Alcázar-Córcoles ,Miguel Ángel, & and Hallak, J. E. C. (2018). Efficacy, tolerability, and safety of serotonergic psychedelics for the management of mood, anxiety, and substance-use disorders: A systematic review of systematic reviews. *Expert Review of Clinical Pharmacology*, *11*(9), 889–902. https://doi.org/10.1080/17512433.2018.1511424

Ekins, T. G., Brooks, I., Kailasa, S., Rybicki-Kler, C., Jedrasiak-Cape, I., Donoho, E., Mashour, G. A., Rech, J., & Ahmed, O. J. (2023). *Cellular rules underlying psychedelic control of prefrontal pyramidal neurons*. bioRxiv. https://doi.org/10.1101/2023.10.20.563334

El Mansari, M., & Blier, P. (1997). In Vivo Electrophysiological Characterization of 5-HT Receptors in the Guinea Pig Head of Caudate Nucleus and Orbitofrontal Cortex. *Neuropharmacology*, *36*(4–5), 577–588. https://doi.org/10.1016/S0028-3908(97)00035-X

El Mansari, M., & Blier, P. (2005). Responsiveness of 5-HT(1A) and 5-HT2 receptors in the rat orbitofrontal cortex after long-term serotonin reuptake inhibition. *Journal of Psychiatry & Neuroscience: JPN*, *30*(4), 268–274.

Elliott, M. C., Tanaka, P. M., Schwark, R. W., & Andrade, R. (2018). Serotonin Differentially Regulates L5 Pyramidal Cell Classes of the Medial Prefrontal Cortex in

Rats and Mice. *Eneuro*, *5*(1), ENEURO.0305-17.2018. https://doi.org/10.1523/ENEURO.0305-17.2018

Escohotado, A. (2005). *Historia General de las Drogas* (5th ed.). Espasa Calpe.

Gener, T., Tauste Campo, A., Alemany-González, M., Nebot, P., Delgado-Sallent, C., Chanovas, J., & Puig, M. V. (2019). Serotonin 5-HT1A, 5-HT2A and dopamine D2 receptors strongly influence prefronto-hippocampal neural networks in alert mice: Contribution to the actions of risperidone. *Neuropharmacology*, *158*, 107743. https://doi.org/10.1016/j.neuropharm.2019.107743

Ghaw, A., Chunduri, A., Chang, A., Ortiz, R. J., Kozlowska, M., Kulkarni, P. P., & Ferris, C. F. (2024). Dose-dependent LSD effects on cortical/thalamic and cerebellar activity: Brain oxygen level–dependent fMRI study in awake rats. *Brain Communications*, *6*(3), fcae194. https://doi.org/10.1093/braincomms/fcae194

Godbout, R., Mantz, J., Glowinski, J., & Thierry, A. M. (1991). The novel 5-HT2 receptor antagonist, RP 62203, selectively blocks serotoninergic but not dopaminergic-induced inhibition in the rat prefrontal cortex. *European Journal of Pharmacology*, *204*(1), 97–100. https://doi.org/10.1016/0014-2999(91)90840-m

González-Maeso, J., Weisstaub, N. V., Zhou, M., Chan, P., Ivic, L., Ang, R., Lira, A., Bradley-Moore, M., Ge, Y., Zhou, Q., Sealfon, S. C., & Gingrich, J. A. (2007). Hallucinogens Recruit Specific Cortical 5-HT2A Receptor-Mediated Signaling Pathways to Affect Behavior. *Neuron*, *53*(3), 439–452. https://doi.org/10.1016/j.neuron.2007.01.008

Goodwin, G. M., Aaronson, S. T., Alvarez, O., Arden, P. C., Baker, A., Bennett, J. C., Bird, C., Blom, R. E., Brennan, C., Brusch, D., Burke, L., Campbell-Coker, K., Carhart-Harris, R., Cattell, J., Daniel, A., DeBattista, C., Dunlop, B. W., Eisen, K., Feifel, D., … Malievskaia, E. (2022). Single-Dose Psilocybin for a Treatment-Resistant Episode of Major Depression. *The New England Journal of Medicine*, *387*(18), 1637–1648. https://doi.org/10.1056/NEJMoa2206443

Groc, L., Heine, M., Cousins, S. L., Stephenson, F. A., Lounis, B., Cognet, L., & Choquet, D. (2006). NMDA receptor surface mobility depends on NR2A-2B subunits.

Proceedings of the National Academy of Sciences, *103*(49), 18769–18774. https://doi.org/10.1073/pnas.0605238103

Hansen, I. H., Agerskov, C., Arvastson, L., Bastlund, J. F., Sørensen, H. B. D., & Herrik, K. F. (2019). Pharmaco-electroencephalographic responses in the rat differ between active and inactive locomotor states. *European Journal of Neuroscience*, *50*(2), 1948–1971. https://doi.org/10.1111/ejn.14373

Haddaway, N. R., Page, M. J., Pritchard, C. C., & McGuinness, L. A. (2022). PRISMA2020: An R package and Shiny app for producing PRISMA 2020-compliant flow diagrams, with interactivity for optimised digital transparency and Open Synthesis. *Campbell Systematic Reviews*, *18*(2), e1230. https://doi.org/10.1002/cl2.1230

Heiss, W.-D., Hoyer, J., & Poustka, F. (1973). Participation of retinal mechanisms in DMT hallucinations. *Experientia*, *29*(4), 455–457. https://doi.org/10.1007/BF01926779

Herzog, R., Mediano, P. A. M., Rosas, F. E., Lodder, P., Carhart-Harris, R., Perl, Y. S., Tagliazucchi, E., & Cofre, R. (2023). A whole-brain model of the neural entropy increase elicited by psychedelic drugs. *Scientific Reports*, *13*(1), 6244. https://doi.org/10.1038/s41598-023-32649-7

Huels, E. R., Kolbman, N., Fields, C. W., Nelson, A. G., Jackson, H., Liu, T., Mashour, G. A., & Pal, D. (2025). *Psychedelic-mediated Reversal of General Anesthesia and Restoration of Brain Dynamics in Rat* (p. 2025.01.22.632279). bioRxiv. https://doi.org/10.1101/2025.01.22.632279

Inserra, A., De Gregorio, D., Rezai, T., Lopez-Canul, M. G., Comai, S., & Gobbi, G. (2021). Lysergic acid diethylamide differentially modulates the reticular thalamus, mediodorsal thalamus, and infralimbic prefrontal cortex: An in vivo electrophysiology study in male mice. *Journal of Psychopharmacology (Oxford, England)*, *35*(4), 469–482. https://doi.org/10.1177/0269881121991569

Irrmischer, M., Aqil, M., Luan, L., Wang, T., Engelbregt, H., Carhart-Harris, R., Linkenkaer-Hansen, K., & Timmermann, C. (2025). *DMT-induced shifts in criticality correlate with ego-dissolution* (p. 2025.02.08.636868). bioRxiv. https://doi.org/10.1101/2025.02.08.636868

Kłodzinska, A., Bijak, M., Tokarski, K., & Pilc, A. (2002). Group II mGlu receptor agonists inhibit behavioural and electrophysiological effects of DOI in mice. *Pharmacology Biochemistry and Behavior*, *73*(2), 327–332. https://doi.org/10.1016/S0091-3057(02)00845-6

Kringelbach, M. L., Cruzat, J., Cabral, J., Knudsen, G. M., Carhart-Harris, R., Whybrow, P. C., Logothetis, N. K., & Deco, G. (2020). Dynamic coupling of whole-brain neuronal and neurotransmitter systems. *Proceedings of the National Academy of Sciences*, *117*(17), 9566–9576. https://doi.org/10.1073/pnas.1921475117

Kurrasch-Orbaugh, D. M., Parrish, J. C., Watts, V. J., & Nichols, D. E. (2003). A complex signaling cascade links the serotonin2A receptor to phospholipase A2 activation: The involvement of MAP kinases. *Journal of Neurochemistry*, *86*(4), 980–991. https://doi.org/10.1046/j.1471-4159.2003.01921.x

Lambe, E. K., & Aghajanian, G. K. (2006). Hallucinogen-Induced UP States in the Brain Slice of Rat Prefrontal Cortex: Role of Glutamate Spillover and NR2B-NMDA Receptors. *Neuropsychopharmacology*, *31*(8), 1682–1689. https://doi.org/10.1038/sj.npp.1300944

Lambe, E. K., & Aghajanian, G. K. (2007). Prefrontal cortical network activity: Opposite effects of psychedelic hallucinogens and D1/D5 dopamine receptor activation. *Neuroscience*, *145*(3), 900–910. https://doi.org/10.1016/j.neuroscience.2006.12.048

Larkum, M. E. (2022). Are Dendrites Conceptually Useful? *Neuroscience*, *489*, 4–14. https://doi.org/10.1016/j.neuroscience.2022.03.008

Luppi, A. I., Carhart-Harris, R. L., Roseman, L., Pappas, I., Menon, D. K., & Stamatakis, E. A. (2021). LSD alters dynamic integration and segregation in the human brain. *NeuroImage*, *227*, 117653. https://doi.org/10.1016/j.neuroimage.2020.117653

Ly, C., Greb, A. C., Cameron, L. P., Wong, J. M., Barragan, E. V., Wilson, P. C., Burbach, K. F., Soltanzadeh Zarandi, S., Sood, A., Paddy, M. R., Duim, W. C., Dennis, M. Y., McAllister, A. K., Ori-McKenney, K. M., Gray, J. A., & Olson, D. E. (2018). Psychedelics Promote Structural and Functional Neural Plasticity. *Cell Reports*, *23*(11), 3170–3182. https://doi.org/10.1016/j.celrep.2018.05.022

Marek, G. J., & Ramos, B. P. (2018). β2-Adrenergic Receptor Activation Suppresses the Rat Phenethylamine Hallucinogen-Induced Head Twitch Response: Hallucinogen-Induced Excitatory Post-synaptic Potentials as a Potential Substrate. *Frontiers in Pharmacology*, *9*, 89. https://doi.org/10.3389/fphar.2018.00089

Martin, D. A., & Nichols, C. D. (2016). Psychedelics Recruit Multiple Cellular Types and Produce Complex Transcriptional Responses Within the Brain. *EBioMedicine*, *11*, 262–277. https://doi.org/10.1016/j.ebiom.2016.08.049

McKay, S., Bengtson, C. P., Bading, H., Wyllie, D. J. A., & Hardingham, G. E. (2013). Recovery of NMDA receptor currents from MK-801 blockade is accelerated by Mg2+ and memantine under conditions of agonist exposure. *Neuropharmacology*, *74*, 119–125. https://doi.org/10.1016/j.neuropharm.2013.01.024

Michaiel, A. M., Parker, P. R. L., & Niell, C. M. (2019). A Hallucinogenic Serotonin-2A Receptor Agonist Reduces Visual Response Gain and Alters Temporal Dynamics in Mouse V1. *Cell Reports*, *26*(13), 3475-3483.e4. https://doi.org/10.1016/j.celrep.2019.02.104

Muir, J., Lin, S., Aarrestad, I. K., Daniels, H. R., Ma, J., Tian, L., Olson, D. E., & Kim, C. K. (2024). Isolation of psychedelic-responsive neurons underlying anxiolytic behavioral states. *Science*, *386*(6723), 802–810. https://doi.org/10.1126/science.adl0666

Muttoni, S., Ardissino, M., & John, C. (2019). Classical psychedelics for the treatment of depression and anxiety: A systematic review. *Journal of Affective Disorders*, *258*, 11–24. https://doi.org/10.1016/j.jad.2019.07.076

Nardai, S., László, M., Szabó, A., Alpár, A., Hanics, J., Zahola, P., Merkely, B., Frecska, E., & Nagy, Z. (2020). N,N-dimethyltryptamine reduces infarct size and improves functional recovery following transient focal brain ischemia in rats. *Experimental Neurology*, *327*, 113245. https://doi.org/10.1016/j.expneurol.2020.113245

Nichols, D. E. (2016). Psychedelics. *Pharmacological Reviews*, *68*(2), 264–355. https://doi.org/10.1124/pr.115.011478

Nocjar, C., Alex, K. D., Sonneborn, A., Abbas, A. I., Roth, B. L., & Pehek, E. A. (2015). Serotonin-2C and -2a receptor co-expression on cells in the rat medial prefrontal

cortex. *Neuroscience*, *297*, 22–37. https://doi.org/10.1016/j.neuroscience.2015.03.050

O'Leary, H., Liu, W. H., Rorabaugh, J. M., Coultrap, S. J., & Bayer, K. U. (2011). Nucleotides and Phosphorylation Bi-directionally Modulate Ca2+/Calmodulin-dependent Protein Kinase II (CaMKII) Binding to the N-Methyl-d-aspartate (NMDA) Receptor Subunit GluN2B. *Journal of Biological Chemistry*, *286*(36), 31272–31281. https://doi.org/10.1074/jbc.M111.233668

Phillips, W. A., Bachmann, T., Spratling, M. W., Muckli, L., Petro, L. S., & Zolnik, T. (2025). Cellular psychology: Relating cognition to context-sensitive pyramidal cells. *Trends in Cognitive Sciences*, *29*(1), 28–40. https://doi.org/10.1016/j.tics.2024.09.002

Poulie, C. B. M., Jensen, A. A., Halberstadt, A. L., & Kristensen, J. L. (2020). DARK Classics in Chemical Neuroscience: NBOMes. *ACS Chemical Neuroscience*, *11*(23), 3860–3869. https://doi.org/10.1021/acschemneuro.9b00528

Puig, M. V., Celada, P., Díaz-Mataix, L., & Artigas, F. (2003). In vivo modulation of the activity of pyramidal neurons in the rat medial prefrontal cortex by 5-HT2A receptors: Relationship to thalamocortical afferents. *Cerebral Cortex (New York, N.Y.: 1991)*, *13*(8), 870–882. https://doi.org/10.1093/cercor/13.8.870

Puigseslloses, P., Nadal-Gratacós, N., Ketsela, G., Weiss, N., Berzosa, X., Estrada-Tejedor, R., Islam, M. N., Holy, M., Niello, M., Pubill, D., Camarasa, J., Escubedo, E., Sitte, H. H., & López-Arnau, R. (2024). Structure-activity relationships of serotonergic 5-MeO-DMT derivatives: Insights into psychoactive and thermoregulatory properties. *Molecular Psychiatry*, *29*(8), 2346–2358. https://doi.org/10.1038/s41380-024-02506-8

Raison, C. L., Sanacora, G., Woolley, J., Heinzerling, K., Dunlop, B. W., Brown, R. T., Kakar, R., Hassman, M., Trivedi, R. P., Robison, R., Gukasyan, N., Nayak, S. M., Hu, X., O'Donnell, K. C., Kelmendi, B., Sloshower, J., Penn, A. D., Bradley, E., Kelly, D. F., … Griffiths, R. R. (2023). Single-Dose Psilocybin Treatment for Major Depressive Disorder: A Randomized Clinical Trial. *JAMA*, *330*(9), 843–853. https://doi.org/10.1001/jama.2023.14530

Riga, M. S., Bortolozzi, A., Campa, L., Artigas, F., & Celada, P. (2016). The serotonergic hallucinogen 5-methoxy-N,N-dimethyltryptamine disrupts cortical activity in a regionally-selective manner via 5-HT(1A) and 5-HT(2A) receptors. *Neuropharmacology*, *101*, 370–378. https://doi.org/10.1016/j.neuropharm.2015.10.016

Riga, M. S., Lladó-Pelfort, L., Artigas, F., & Celada, P. (2018). The serotonin hallucinogen 5-MeO-DMT alters cortico-thalamic activity in freely moving mice: Regionally-selective involvement of 5-HT1A and 5-HT2A receptors. *Neuropharmacology*, *142*, 219–230. https://doi.org/10.1016/j.neuropharm.2017.11.049

Riga, M. S., Soria, G., Tudela, R., Artigas, F., & Celada, P. (2014). The natural hallucinogen 5-MeO-DMT, component of Ayahuasca, disrupts cortical function in rats: Reversal by antipsychotic drugs. *The International Journal of Neuropsychopharmacology*, *17*(08), 1269–1282. https://doi.org/10.1017/S1461145714000261

Rueter, L. E., & Blier, P. (1999). Electrophysiological examination of the effects of sustained flibanserin administration on serotonin receptors in rat brain. *British Journal of Pharmacology*, *126*(3), 627–638. https://doi.org/10.1038/sj.bjp.0702344

Reuter, L. E., Tecott, L. H., & Blier, P. (2000). In vivo electrophysiological examination of 5-HT2 responses in 5-HT2C receptor mutant mice. *Naunyn-Schmiedeberg's Archives of Pharmacology*, *361*(5). https://doi.org/10.1007/s002109900181

Schimmers, N., Breeksema, J. J., Smith-Apeldoorn, S. Y., Veraart, J., van den Brink, W., & Schoevers, R. A. (2022). Psychedelics for the treatment of depression, anxiety, and existential distress in patients with a terminal illness: A systematic review. *Psychopharmacology*, *239*(1), 15–33. https://doi.org/10.1007/s00213-021-06027-y

Schmidt, M., Hoffrichter, A., Davoudi, M., Horschitz, S., Lau, T., Meinhardt, M., Spanagel, R., Ladewig, J., Köhr, G., & Koch, P. (2024). *Psilocin fosters neuroplasticity in iPSC-derived human cortical neurons*. In Review. https://doi.org/10.21203/rs.3.rs-4242829/v1

Schmitz, G. P., Chiu, Y.-T., König, G. M., Kostenis, E., Roth, B. L., & Herman, M. A. (2022). *Psychedelic compounds directly excite 5-HT2A Layer 5 Pyramidal Neurons*

in the Prefrontal Cortex through a 5-HT2A Gq -mediated activation mechanism. bioRxiv. https://doi.org/10.1101/2022.11.15.516655

Shao, L.-X., Liao, C., Davoudian, P. A., Savalia, N. K., Jiang, Q., Wojtasiewicz, C., Tan, D., Nothnagel, J. D., Liu, R.-J., Woodburn, S. C., Bilash, O. M., Kim, H., Che, A., & Kwan, A. C. (2025). Psilocybin's lasting action requires pyramidal cell types and 5-HT2A receptors. *Nature*, 1–10. https://doi.org/10.1038/s41586-025-08813-6

Shao, L.-X., Liao, C., Gregg, I., Davoudian, P. A., Savalia, N. K., Delagarza, K., & Kwan, A. C. (2021). Psilocybin induces rapid and persistent growth of dendritic spines in frontal cortex in vivo. *Neuron*, *109*(16), 2535-2544.e4. https://doi.org/10.1016/j.neuron.2021.06.008

Smausz, R., Neill, J., & Gigg, J. (2022). Neural mechanisms underlying psilocybin's therapeutic potential – the need for preclinical in vivo electrophysiology. *Journal of Psychopharmacology*, *36*(7), 781–793. https://doi.org/10.1177/02698811221092508

Souza, A. C., Souza, B. C., França, A., Moradi, M., Souza, N. C., Leão, K. E., Tort, A. B. L., Leão, R. N., Lopes-Dos-Santos, V., & Ribeiro, S. (2024). 5-MeO-DMT induces sleep-like LFP spectral signatures in the hippocampus and prefrontal cortex of awake rats. *Scientific Reports*, *14*(1), 11281. https://doi.org/10.1038/s41598-024-61474-9

Spindle, M. S., & Thomas, M. P. (2014). Activation of 5-HT2A receptors by TCB-2 induces recurrent oscillatory burst discharge in layer 5 pyramidal neurons of the mPFC in vitro. *Physiological Reports*, *2*(5), e12003. https://doi.org/10.14814/phy2.12003

Squire, L., Berg, D., Bloom, F. E., Lac, S. du, Ghosh, A., & Spitzer, N. C. (2012). *Fundamental Neuroscience*. Academic Press.

Stutzmann, G. E., Marek, G. J., & Aghajanian, G. K. (2001). Adenosine preferentially suppresses serotonin2A receptor-enhanced excitatory postsynaptic currents in layer V neurons of the rat medial prefrontal cortex. *Neuroscience*, *105*(1), 55–69. https://doi.org/10.1016/S0306-4522(01)00170-1

Suzuki, M., & Larkum, M. E. (2020). General Anesthesia Decouples Cortical Pyramidal Neurons. *Cell*, *180*(4), 666-676.e13. https://doi.org/10.1016/j.cell.2020.01.024

Szabo, A., Kovacs, A., Riba, J., Djurovic, S., Rajnavolgyi, E., & Frecska, E. (2016). The Endogenous Hallucinogen and Trace Amine N,N-Dimethyltryptamine (DMT) Displays Potent Protective Effects against Hypoxia via Sigma-1 Receptor Activation in Human Primary iPSC-Derived Cortical Neurons and Microglia-Like Immune Cells. *Frontiers in Neuroscience*, *10*, 423. https://doi.org/10.3389/fnins.2016.00423

Szabó, Í., Varga, V. É., Dvorácskó, S., Farkas, A. E., Körmöczi, T., Berkecz, R., Kecskés, S., Menyhárt, Á., Frank, R., Hantosi, D., Cozzi, N. V., Frecska, E., Tömböly, C., Krizbai, I. A., Bari, F., & Farkas, E. (2021). N,N-Dimethyltryptamine attenuates spreading depolarization and restrains neurodegeneration by sigma-1 receptor activation in the ischemic rat brain. *Neuropharmacology*, *192*, 108612. https://doi.org/10.1016/j.neuropharm.2021.108612

Tanaka, E., & North, R. A. (1993). Actions of 5-hydroxytryptamine on neurons of the rat cingulate cortex. *Journal of Neurophysiology*, *69*(5), 1749–1757. https://doi.org/10.1152/jn.1993.69.5.1749

Thomas, C. W., Blanco-Duque, C., Bréant, B. J., Goodwin, G. M., Sharp, T., Bannerman, D. M., & Vyazovskiy, V. V. (2022). Psilocin acutely alters sleep-wake architecture and cortical brain activity in laboratory mice. *Translational Psychiatry*, *12*(1), 77. https://doi.org/10.1038/s41398-022-01846-9

Troca-Marín, J. A., & Geijo-Barrientos, E. (2010). Inhibition by 5-HT of the synaptic responses evoked by callosal fibers on cortical neurons in the mouse. *Pflugers Archiv: European Journal of Physiology*, *460*(6), 1073–1085. https://doi.org/10.1007/s00424-010-0875-4

van Elk, M., & Yaden, D. B. (2022). Pharmacological, neural, and psychological mechanisms underlying psychedelics: A critical review. *Neuroscience and biobehavioral reviews*, *140*, 104793. https://doi.org/10.1016/j.neubiorev.2022.104793

Vicini, S., Wang, J. F., Li, J. H., Zhu, W. J., Wang, Y. H., Luo, J. H., Wolfe, B. B., & Grayson, D. R. (1998). Functional and Pharmacological Differences Between Recombinant *N* -Methyl- D -Aspartate Receptors. *Journal of Neurophysiology*, *79*(2), 555–566. https://doi.org/10.1152/jn.1998.79.2.555

Villalobos, C., Beique, J., Gingrich, J. A., & Andrade, R. (2005). Serotonergic regulation of calcium-activated potassium currents in rodent prefrontal cortex. *European Journal*

of Neuroscience, *22*(5), 1120–1126. https://doi.org/10.1111/j.1460-9568.2005.04307.x

Vollenweider, F. X., & Geyer, M. A. (2001). A systems model of altered consciousness: Integrating natural and drug-induced psychoses. *Brain Research Bulletin*, *56*(5), 495–507. https://doi.org/10.1016/s0361-9230(01)00646-3

Vollenweider, F. X., & Preller, K. H. (2020). Psychedelic drugs: Neurobiology and potential for treatment of psychiatric disorders. *Nature Reviews Neuroscience*, *21*(11), 611–624. https://doi.org/10.1038/s41583-020-0367-2

von Rotz, R., Schindowski, E. M., Jungwirth, J., Schuldt, A., Rieser, N. M., Zahoranszky, K., Seifritz, E., Nowak, A., Nowak, P., Jäncke, L., Preller, K. H., & Vollenweider, F. X. (2023). Single-dose psilocybin-assisted therapy in major depressive disorder: A placebo-controlled, double-blind, randomised clinical trial. *EClinicalMedicine*, *56*, 101809. https://doi.org/10.1016/j.eclinm.2022.101809

Wang, Y., Kristensen, J. L., & Kohlmeier, K. A. (2025). The Selective 5HT2A Receptor Agonist, 25CN-NBOH Exerts Excitatory and Inhibitory Cellular Actions on Mouse Medial Prefrontal Cortical Neurons. *Synapse (New York, N.Y.)*, *79*(2), e70014. https://doi.org/10.1002/syn.70014Weber, E. T., & Andrade, R. (2010). Htr2a Gene and 5-HT(2A) Receptor Expression in the Cerebral Cortex Studied Using Genetically Modified Mice. *Frontiers in Neuroscience*, *4*, 36. https://doi.org/10.3389/fnins.2010.00036

Wojtas, A., Bysiek, A., Wawrzczak-Bargiela, A., Szych, Z., Majcher-Maślanka, I., Herian, M., Maćkowiak, M., & Gołembiowska, K. (2022). Effect of Psilocybin and Ketamine on Brain Neurotransmitters, Glutamate Receptors, DNA and Rat Behavior. *International Journal of Molecular Sciences*, *23*(12), 6713. https://doi.org/10.3390/ijms23126713

Wood, J., Kim, Y., & Moghaddam, B. (2012). Disruption of Prefrontal Cortex Large Scale Neuronal Activity by Different Classes of Psychotomimetic Drugs. *The Journal of Neuroscience*, *32*(9), 3022–3031. https://doi.org/10.1523/JNEUROSCI.6377-11.2012

Woolfrey, K. M., O'Leary, H., Goodell, D. J., Robertson, H. R., Horne, E. A., Coultrap, S. J., Dell'Acqua, M. L., & Bayer, K. U. (2018). CaMKII regulates the depalmitoylation and synaptic removal of the scaffold protein AKAP79/150 to mediate structural long-term depression. *Journal of Biological Chemistry*, *293*(5), 1551–1567. https://doi.org/10.1074/jbc.M117.813808

Zhai, Y., George, C. A., Zhai, J., Nisenbaum, E. S., Johnson, M. P., & Nisenbaum, L. K. (2003). Group II metabotropic glutamate receptor modulation of DOI-induced c-fos mRNA and excitatory responses in the cerebral cortex. *Neuropsychopharmacology: Official Publication of the American College of Neuropsychopharmacology*, *28*(1), 45–52. https://doi.org/10.1038/sj.npp.1300013

Zhou, D., Schuler, H., Cvetkovska, V., Meccia, J., Harutyunyan, A. S., Ragoussis, J., & Bagot, R. C. (2025). *Single-cell sequencing reveals psilocybin induces sustained cell-type specific plasticity in mouse medial prefrontal cortex* (p. 2025.01.08.631940). bioRxiv. https://doi.org/10.1101/2025.01.08.631940

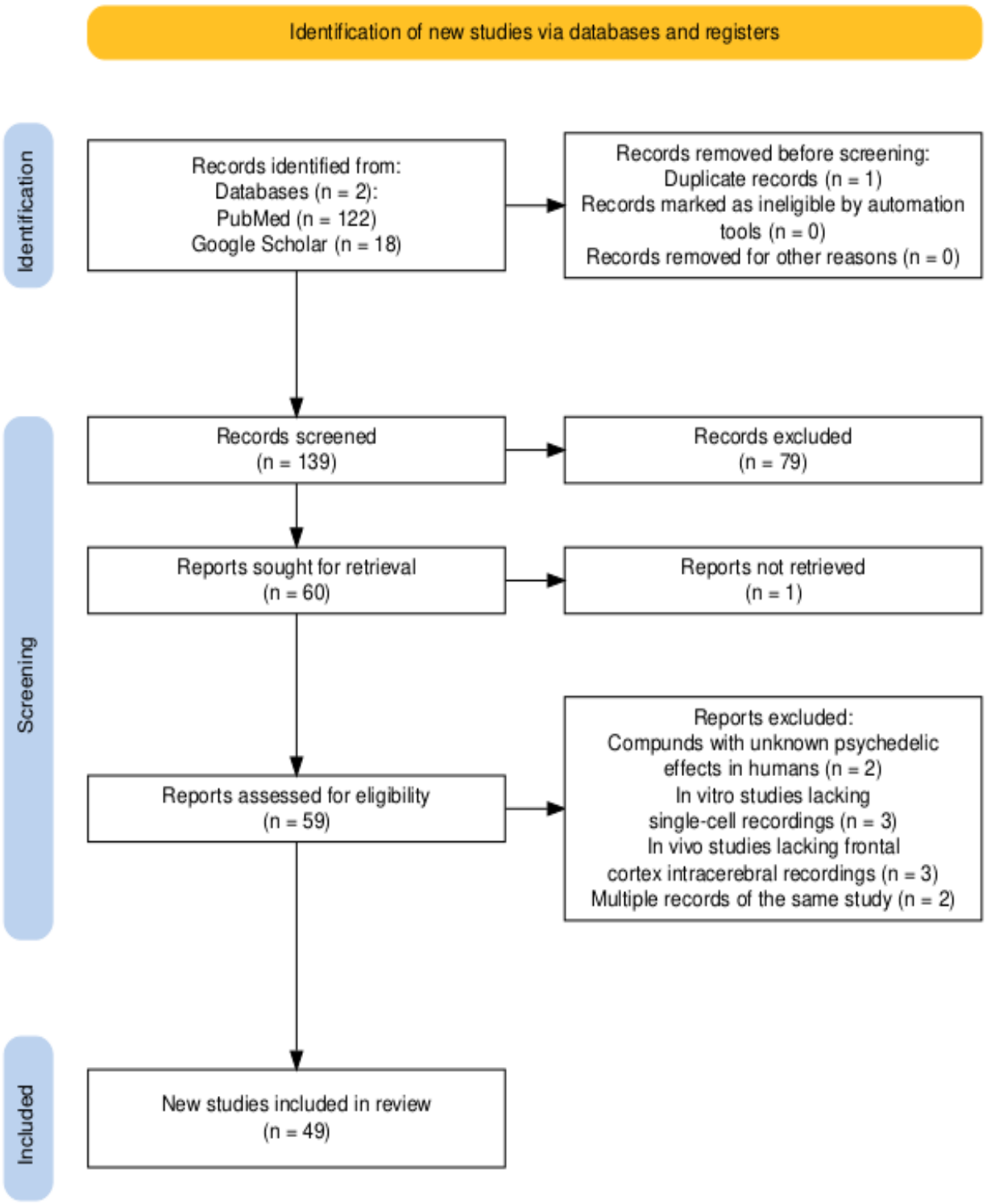

Figure 1: PRISMA flow diagram for study selection.

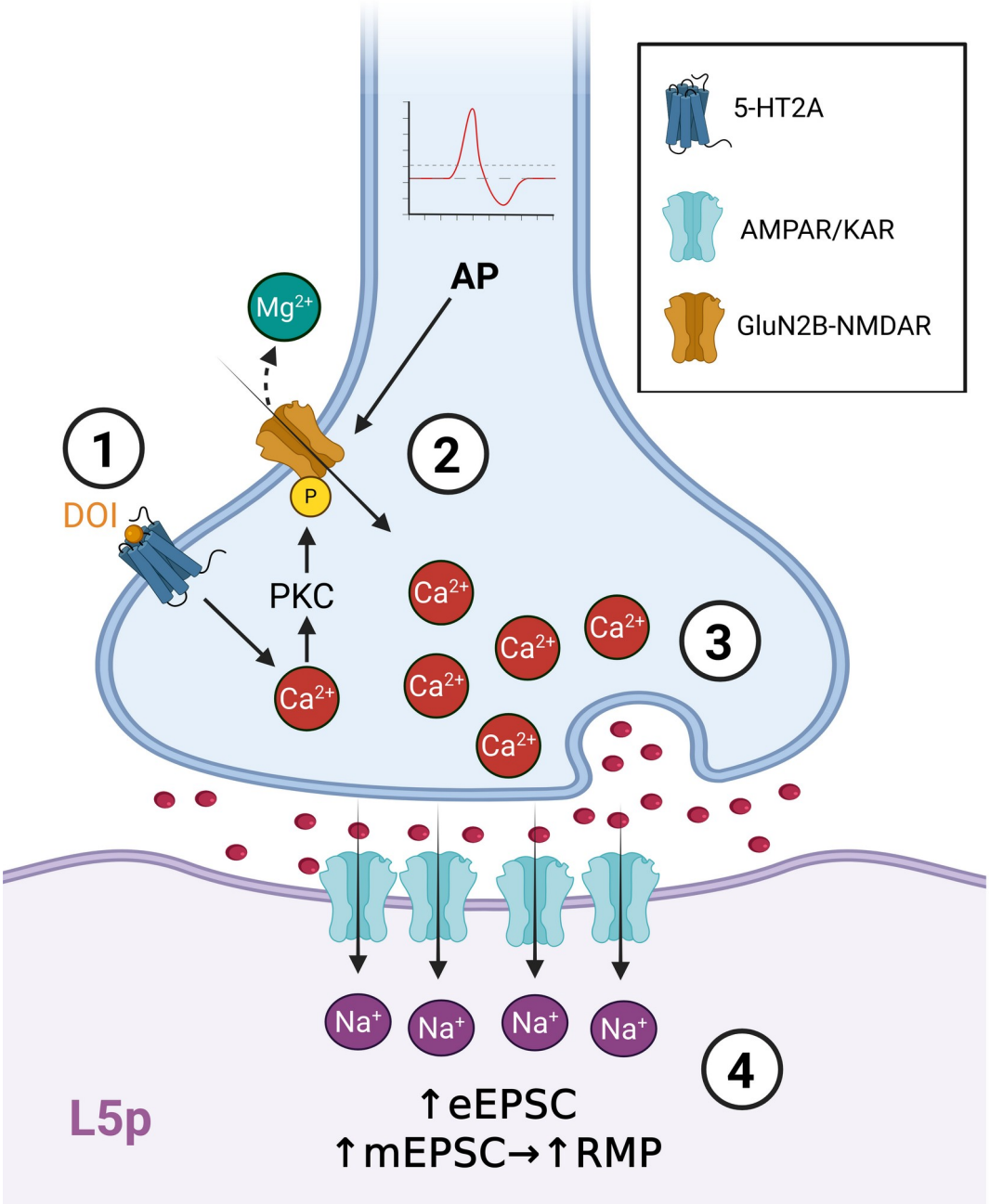

Figure 2: Early Response to DOI. Psychedelics lacking affinity for the 5-HT1A receptor can elicit an early excitatory response at low doses. Here, 2,5-dimethoxy-4-iodoamphetamine (DOI) is illustrated as a prototypical 5-HT2A-selective psychedelic. **1.** DOI binds to presynaptic 5-HT2A receptors, activating protein kinase C (PKC), which in turn phosphorylates GluN2B-containing NMDA receptors (GluN2B-NMDARs), enhancing their conductance. **2.** Upon the arrival of an action potential, the Mg^{2+} block is relieved from the NMDARs, allowing Ca^{2+} ions to enter the presynaptic terminal. **3.** Elevated presynaptic Ca^{2+} levels increase glutamate release (Red dots) into the synaptic cleft, activating postsynaptic AMPA and kainate receptors (AMPARs/KARs). Synchronous activation increases the amplitude of evoked excitatory postsynaptic currents (eEPSCs), while asynchronous activation increases the frequency of miniature excitatory postsynaptic currents (mEPSCs), contributing to a rise in the resting membrane potential (RMP).

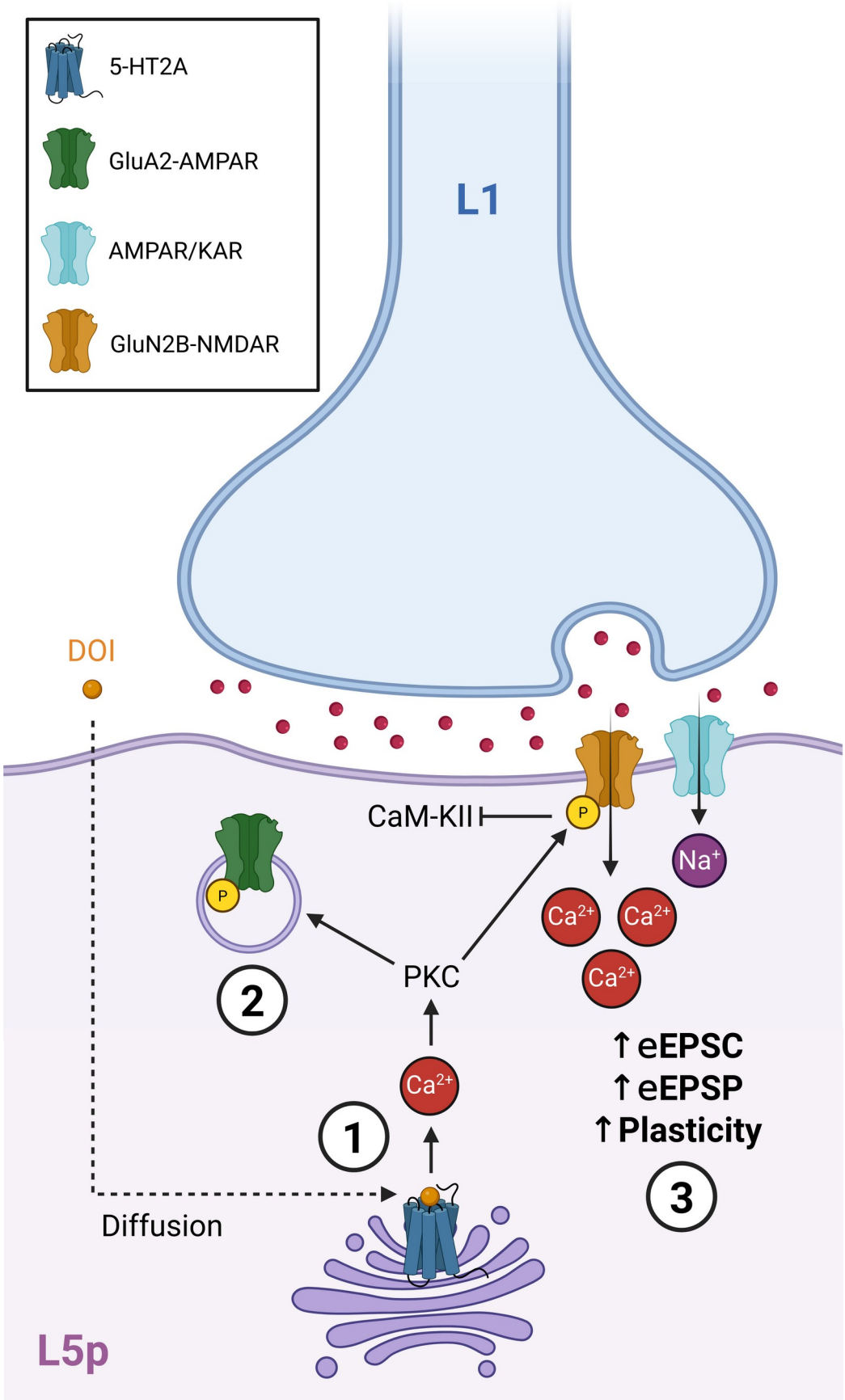

Figure 3: Late Response to DOI in Apical Tuft Dendrites. Psychedelics lacking affinity for the 5-HT1A receptor elicit a late excitatory response at low doses in the tuft dendrites of layer 5 pyramidal neurons. Here, 2,5-dimethoxy-4-iodoamphetamine (DOI) is illustrated as a

prototypical 5-HT2A-selective psychedelic. **1.** DOI diffuses through the postsynaptic membrane, reaching intracellular 5-HT2A receptors, where activation recruits protein kinase C (PKC) via Ca^{2+}-dependent signaling. **2.** PKC phosphorylates GluA2-containing AMPA receptors (GluA2-AMPARs), promoting their internalization and reducing AMPA-mediated transmission. **3.** At the same time, PKC phosphorylates GluN2B-containing NMDA receptors (GluN2B-NMDARs), enhancing their conductance and preventing modulation by Ca^{2+}/calmodulin-dependent protein kinase II (CaM-KII). The activation of AMPA and kainate receptors (AMPARs/KAR) allows Ca^{2+} entry through GluN2B-NMDAR, boosting excitatory postsynaptic currents (EPSCs) and promoting structural plasticity.

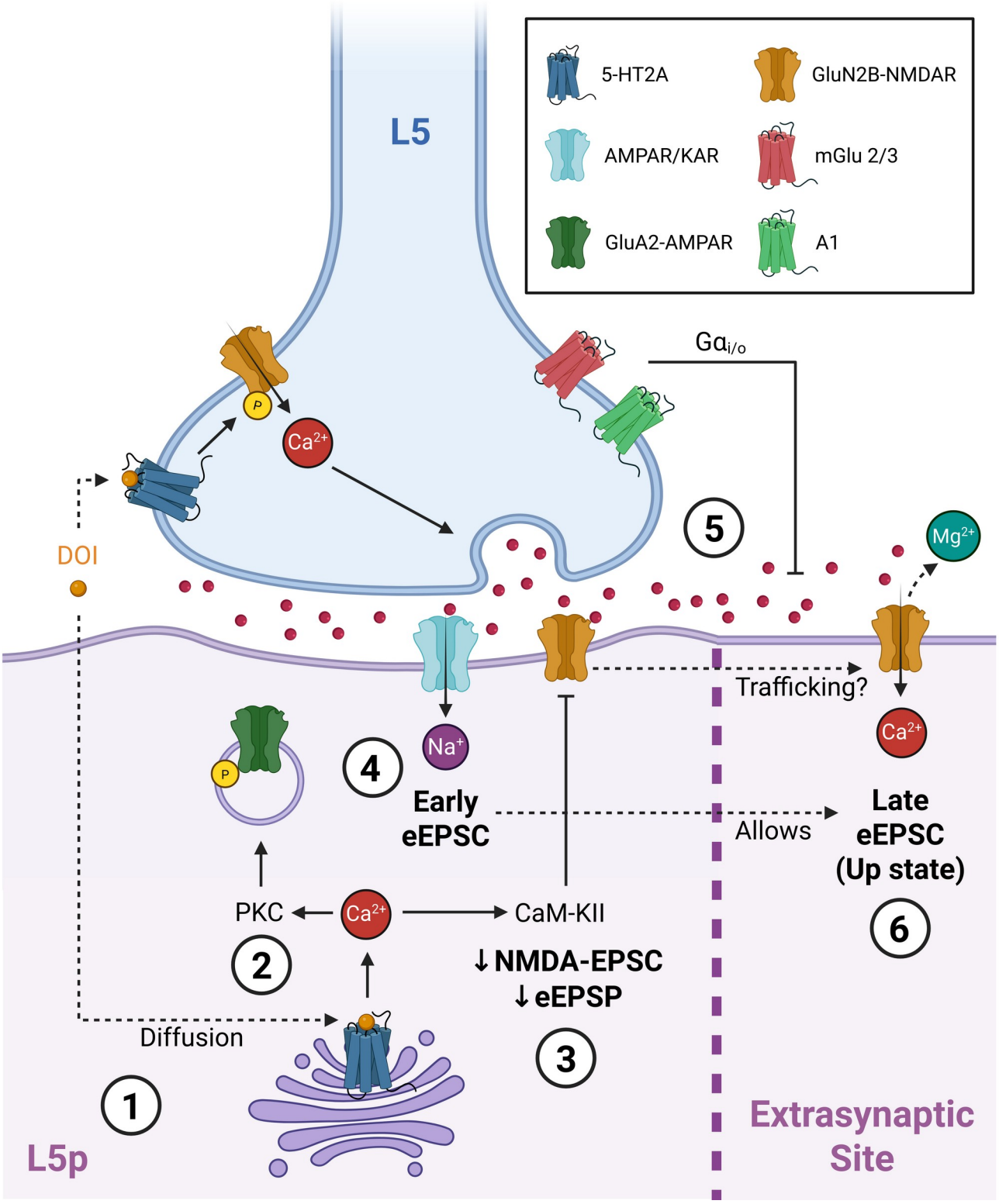

Figure 4: Late Response to DOI in Basal Dendrites. Psychedelics lacking affinity for the 5-HT1A receptor elicit a complex late response at low doses in basal dendrites of layer 5 pyramidal neurons. Here, 2,5-dimethoxy-4-iodoamphetamine (DOI) is illustrated as a prototypical 5-HT2A-selective psychedelic. 1. DOI diffuses through the postsynaptic membrane, reaching intracellular 5-HT2A receptors and triggering Ca^{2+} signaling. 2. Ca2+ activates protein kinase C (PKC), which phosphorylates GluA2-containing AMPA receptors (GluA2-AMPARs), promoting their internalization and reducing AMPA-mediated transmission. 3. Concurrently, Ca^{2+}/calmodulin-dependent protein kinase II (CaM-KII) is activated and facilitates the trafficking of GluN2B-containing NMDA receptors (GluN2B-

NMDARs), reducing NMDA-mediated transmission. 4. Upon glutamate release (Red dots), postsynaptic AMPA and kainate receptors (AMPAR/KAR) are activated, producing an early (synchronous) evoked excitatory postsynaptic current (eEPSC). 5. Glutamate spillover, driven by presynaptic 5-HT2A receptor activation and GluN2B-NMDAR phosphorylation, is modulated by presynaptic metabotropic glutamate receptors 2/3 (mGlu 2/3) and the adenosine A1 receptor (A1). 6. The trafficking of GluN2B-NMDARs may increase the excitability of extrasynaptic sites. The diffusion of the early eEPSC to extrasynaptic regions removes the Mg^{2+} block from GluN2B-NMDAR, which are activated by glutamate spillover. They elicit a late eEPSC associated with transient up states, increasing the resting membrane potential.

Table 1: *In vitro* studies

Specie	Region	Drug	Concentration	Membrane Properties	Postsynaptic Activity	Action Potentials	Other Findings	Reference	Peer-Review
Rat	ACC, mPFC	DOB	3-30 μM	**RMP**: Slowly developing depolarization		**Number of spikes**: Elicited by a depolarizing pulse. marked increase.	Slow onset, lasted minutes after drug removal. Antagonized by ketanserin.	Araneda & Andrade, 1991	Yes
						Frequency adaptation: Decreas e			
						AHP: Gradual replacement by slow depolarizing afterpotential following spike train.			
Rat	ACC	DOI	10 μM	**RMP**: Slowly developing depolarization	**eEPSP**: Evoked by electrical stimulation of forceps minor or L5. No reduction in amplitude.		5-HT reduced the amplitude of EPSPs.	Tanaka & North, 1993	Yes
Rat	Frontal neocortex	DOI	3-10 μM		**eEPSP**: Evoked by electrical stimulation of L1. Increased amplitude.		In the same cells, 5-HT depressed eEPSPs. Focal microiontophoretic 5-HT in L4/5a, but not in basal dendrites of L5p, elicited EPSCs in all cells.	Aghajanian & Marek, 1997	Yes
					SEPSC: Small increase in frequency.		TTX (2 μM) blocked 5-HT (100 μM) -induced sEPSCs.		
							Exposures longer than 1-2 min sometimes resulted in desensitization of the effect.		
Rat	mPFC, AAC	DOI	3 μM		**eEPSC**: Evoked by electrical stimulation of forceps minor. Late eEPSC emerge following rhythmic stimulation (≥0.1 Hz).		M100907 (100 nM) or 5-HT (100 μM) suppressed late component of eEPSC.	Aghajanian & Marek, 1999	Yes
					sEPSC: 90% less increase in frequency than 5-HT.				
Rat	mPFC	DOB	0.01-50 μM	**RMP:** NS at 0.1-20 μM.	**eEPSP**: Evoked by NMDA (10 μM). DOB (0.1 μM) increased	**Duration at half amplitude**: NS change	5-HT + WAY 100635 (0.5 μM; 5-HT1A antagonist) showed	Arvanov et al., 1999a	Yes

					frequency and amplitude.		similar biphasic effects (5-50 μM inhibitory, 100-200 μM excitatory).		
				RMP: +2-5 mV slow depolarization after 15-20 minutes of perfusion at 20 μM.	**eEPSP**: Evoked by electrical stimulation of forceps minor. DOB (0.1 μM): No effect. DOB (1 μM): Increased amplitude (5-15 min), followed by depression in most cells. DOB (20 μM): Decreased amplitude in all cells.	**Amplitude:** NS change	M100907 (10 nM) and ketanserin (100 nM) blocked both facilitatory and inhibitory effects. WAY 100635 or BRL 46470A (5-HT3 antagonist) were ineffective.		
				RMP: +5-8 mV at 30-50 μM.	**eEPSC:** Evoked by NMDA (10 μM). DOB (0.01-1 μM): Dose-dependent facilitation. Strong desensitization after 20 min. DOB (20 μM): Inhibition. Not desensitized after 45 min. Persisted >1.5h post-washout.	**τ:** NS change	Bicuculline (30 μM) plus CGP 52432 (0.5 μM; GABAB antagonist) were ineffective.		
				Ri: NS increase at 0.1 μM, NS decrease at 20 μM.	**eEPSC:** Evoked by AMPA (5 μM). DOB (0.1μM): +25% amplitude in 3/5 cells. DOB (20 μM): +30% amplitude in 7/16 cells.	**sAHP:** Decrease. Prevented by TTX + bicuculline.	CNQX (20 μM) blocked the excitatory action, unmasking the inhibitory effect.		
					eEPSC: Evoked by electrical stimulation of the forceps minor. MK-801-loaded electrodes (0.1 mM). DOB (0.1 μM): enhanced NMDA facilitating action. DOB (20 μM): depressed basal EPSCs and abolished NMDA facilitating action.	**Frequency adaptation:** Dose-dependent decrease. Prevented by TTX and bicuculline.	Intracellular BAPTA (Ca^{2+} chelator) to recorded neuron, W-7 bath (10-30 μM; CaM inhibitor), or KN-93 (1 μM; Ca2+/CaM-KII inhibitor) blocked DOB's inhibitory effect without affecting facilitation.		
						Bursts: Evoked by NMDA (10 μM) with glycine (1 μM). DOB (0.1 μM): increased frequency to 448%. Bicuculline	Chelerythrine (1-5 μM; PKC inhibitor) prevented DOB's facilitatory, but not inhibitory effect.		

						(1 μM) had no significant effect. DOB (20 μM): decreased frequency to 17% in same cells excited by 0.1 μM.			
							BAPTA-AM (30 μM, 30 min; membrane-permeable Ca^{+2} chelator) or thapsigargin (1 μM, 30 min; intracellular IP3-sensitive Ca^{+2} depleter) blocked DOB's facilitatory and inhibitory effects.		
							0.1 μM DOB inhibited NMDA current in various conditions to abolish glutamate release and/or block the non-NMDA component of EPSCs: Ca^{+2}-free ACSF, low Ca^{+2} (0.1 mM) + Cd^{+2} (0.2 mM) ACSF, high Mg^{+2} (5 mM) ACSF, riluzole (50 μM; glutamate-release inhibitor).		
Rat	mPFC	LSD	0.5-2000 nM		**eEPSC:** Evoked by NMDA (10 μM). LSD (0.5-1000 nM): Inhibition. Onset >10 min of continuous perfusion.		M100907 (10 nM) or ketanserin (100 nM) blocked LSD's inhibitory effect.	Arvanov et al., 1999b	Yes
							CNQX (20 μM) blocked LSD+WAY100635 facilitatory effect, unmasking inhibition.		
							Lisuride (non-hallucinogenic LSD analog) produced a monophasic facilitating action. CNQX abolished the facilitating effect of lisuride without unmasking any inhibitory action.		

		DOB	50-500 nM		**eEPSC**: Evoked by NMDA (10 μM). In presence of WAY 100635 (0.5 μM; 5-HT1A antagonist) LSD (0.5-50 nM): Inhibition. LSD (0.5-2 μM): Facilitation. Desensitized after 20 min of continuous LSD (0.5 μM) perfusion, unmasking inhibition.		BL 3912A, a non-hallucinogenic DOB analog, failed to alter the NMDA response consistently.		
					eEPSC: Evoked by electrical stimulation of the forceps minor. In the presence of CNQX (20 μM), holding potential at -40 mV. LSD (50 nM), DOB (500 nM) and 5-HT (50 μM) significantly reduced the peak amplitude of eEPSCs.		Neither lisuride (50 nM) nor BL 3912A (500 nM) affected NMDA modulation of eEPSCs evoked by electrical stimulation of the forceps minor.		
							IC_{50}: LSD (9 nM) < DOB (130 nM) < 5-HT (31 μM). I_{max}: 5-HT (100%) > DOB (82%) > LSD (68%).		
							Chelerythrine (1 μM; PKC inhibitor) did not affect inhibition. W-7 (30 μM; CaM inhibitor) or KN-93 (1 μM; selective Ca+2/CaM-KII inhibitor) blocked inhibition.		
Rat	mPFC	DOI	?		**eEPSC:** Evoked by electrical stimulation of the forceps minor. Enhanced late component of eEPSCs while having only a slight effect on early eEPSCs.		Adenosine (30 μM), CPA (3-300 nM, A1 agonist), AP5 (NMDAR antagonist) and M100907 blocked late eEPSC with little effect on early eEPSC. DPCPX (A1 antagonist) reversed the effect of adenosine.	Stutzmann et al., 2001	Yes
							CNQX completely blocked both the early and the late		

							components.		
Mouse	Frontal cortex	DOI	10 μM		**sEPSP**: After 6-10 min, enhanced frequency by 350%. Effect did not desensitize after 20 min.		Co-application of LY379268 (1 μM; mGlu2/3 agonist) reversibly suppressed EPSPs to control levels or below.	Kłodzinska et al., 2002	Yes
Rat	PFC	DOI	3 μM		**eEPSP**: Evoked by electrical stimulation of the L5. Increased amplitude by 30%.		LY379268 (0.01-1 μM, mGlu 2/3 agonist) suppressed eEPSP increase. LY341495 (1 μM, mGlu2/3 antagonist) blocked LY379268's effect.	Zhai et al., 2003	Yes
Rat	mPFC, ACC	DOB	5-20 μL drop from 1 mM solution	**RMP**: Depolarization of 50% of L5p during postnatal days P6-19. Significant reduction in % cells and response after P14.			Membrane depolarization showed 40% desensitization after second application, 8-12 min apart.	Béïque et al., 2004	Yes
				Ri: Small increase.			Depolarization was blocked by Ketanserin (1 μM) and M100907 (100 nM), but not SB 242084 (100 nM; 5-HT2C antagonist).		
							During P6-19, 5-HT depolarized most cells. DOB depolarized only 50%.		
Rat	mPFC	DOB	?			**AHP:** 44% inhibition of slow component of AHP current (Is_{AHP}).	M100907 (100 nM) blocked the effect.	Villalobos et al., 2005	Yes
Rat	mPFC	DOI	3 μM	**RMP:** NS increase.	**eEPSC**: Evoked by 0.1 Hz electrical stimulation of layers 2/3 or 5. DOI (15 min) or LSD (10 min) elicited late eEPSC lasting up to 2 s after every fast eEPSC. More frequent rates reduce late eEPSC until complete suppression at 1 Hz, while fast EPSC	**Amplitude:** Elicited by a depolarizing pulse. NS increase.	Wash-in of 5% dextran to increase viscosity attenuated late eEPSCs without significantly changing fast eEPSCs, suggesting late wave of glutamate release enhanced by psychedelics stimulates distant extrasynaptic receptors.	Lambe & Aghajanian, 2006	Yes

					persists. Effect lasts >2h after washout.				
		LSD	10 nM	**Ri:** NS increase.		**Number of spikes:** Elicited by a depolarizing pulse. NS increase.	Inhibition of GluN2B-containing NMDAR with Ro25-6981 (500 nM) or ifenprodil (3 μM) suppressed late, but not fast component of eEPSCs.		
							Increasing glutamate spillover with TBOA (30 μM; glutamate transporter inhibitor) + LY341495 (300 nM) enhanced late eEPSCs.		
							LY341495 (300 nM) did not increase DOI-enhanced late eEPSCs.		
							MK-801 in the recording pipette did not prevent late eEPSCs, suggesting the action of extrasynaptic GluN2B-NMDAR.		
Rat	mPFC	DOI	3 μM		**eEPSC**: Evoked by electrical stimulation of the cortical mid-layer. DOI (15 min) enhanced late eEPSC.		Both basal and DOI-enhanced late eEPSC oscillate at the gamma band (30-80 Hz).	Lambe & Aghajanian, 2007	Yes
							SKF 38393 (100 nM; D1/5 agonist) suppressed both basal and DOI-enhanced late eEPSC.		
							In DOI-treated slices, spontaneous late eEPSC by lowering Ca^{+2} and Mg^{+2} from 2 mM to 1 mM. SKF 38393 suppressed the effect.		
							Baseline late eEPSC suppressed by forskolin (10 μM; adenylyl cyclase activator) or 8-Br-cAMP (0.5 mM; phosphodiesterase-		

							resistant cAMP analog)		
							Bicuculline (1 μM) enhanced electrically-evoked late eEPSC.		
							TBOA (6 μM) restored late eEPSC suppressed by SKF 38393 (100 nM). Trans-PDC (6-30 μM; inhibitor of glial glutamate transporters) did not alter SKF 38393 suppression.		
Mouse	ACC (layers 2-5)	DOI	10 μM	**Holding current**: -52 pA	**eEPSC**: Evoked by electrical stimulation of the corpus callosum. Decreased peak amplitude by 25% in 50% of the neurons tested. Reversed after 7-9 min washout.		MDL 11939 (0.5 μM, 5-HT2A antagonist) blocked the effect.	Troca-Marín & Geijo-Barrientos, 2010	Yes
				Membrane conductance: +1 nS	Increased **CV** of eEPSC amplitude's fluctuations, suggesting a presynaptic mechanism.		The difference between DOI alone and DOI + 8-OH-DPAT (10 μM, 5-HT1A agonist) was not statistically significant.		
							Paired-pulse ratio increase suggested decreased release following 5-HT treatment.		
Mouse	mPFC, ACC	TCB-2	10 μM	**RMP**: +4.3 mV		**Bursts**: TCB-2 + bicuculline (10 μM) + DNQX (20 μM). Recurrent oscillatory bursting (ROB) appeared after 15-20 s of tonic spiking evoked by sustained current injection in 50% of the cells tested. Reversed after 5-10 min wash out. ROB did not appear in neurons treated with TCB-2 alone.	ROB was only observed by injecting current that brought neurons to just suprathreshold membrane potentials (max effect at 116% of rheobase). Larger currents increased tonic spiking, but suppressed ROB.	Spindle & Thomas, 2014	Yes
							ROB was blocked by ketanserin (750 nM).		
				Ri: +15.1 MΩ			Neurons displaying		

							ROB exhibited depolarizing larger sags in response to a hyperpolarizing current.		
							In the absence of bicuculline, large (down to -10 mV) IPSPs occurred, suggesting IPSPs biased neurons to tonic spiking.		
Rat	mPFC	DMT	1-10 mg/kg (i.p.)		**sEPSC:** Increased frequency and amplitude 24h after treatment *in vivo*.			Ly et al., 2018	Yes
Mouse (WT and 5-HT2A KO)	mPFC, ACC	DOI	1 μM		**eEPSC:** Evoked by L1 stimulation. Mg^{2+}-free ACSF, NBQX (2 μM), resting potential (nonselective NMDAR isolation). After 20 min, DOI increased eEPSC amplitude. Reversible after washout.		EEPSC increase blocked by ketanserin (1 μM) and absent in 5-HT2A KO mice.	Barre et al., 2016	Yes
					eEPSC: In presence of Mg^{+2} (1 mM) and holding potential of +40 mV (postsynaptic NMDAR isolation). eEPSCs increase was lost, suggesting the engagement of presynaptic NMDARs.		DOI (10 min) decreased paired pulse ratio, suggesting increased presynaptic glutamate release.		
Rat					**mEPSC**: TTX (1 μM), MK-801 (1 μM) in pipette, Mg^{+2}-free. Increased AMPAR mEPSC frequency. Effect abolished with high Mg^{+2} (4 mM) or AP5 (100 μM).		Restoring 5-HT2A in mPFC of 5-HT2A KO mice (postsynaptic rescue) did not rescue DOI-enhanced NMDA eEPSCs.		
							Restoring 5-HT2A in MDN of thalamus (presynaptic rescue) rescued DOI-enhanced NMDA eEPSCs.		
							Bath NPC15437 (20 μM; PKC inhibitor) or U73122 (5 μM; PLC inhibitor) blocked eEPSC increase. GDP-		

							βS (1 mM; G protein inhibitor) or U73122 (5 μM) in pipette had no effect.		
							NPC15437 (20 μM) or BAPTA (20 μM) in pipette: transient eEPSC increase, returned to baseline in 15-20 min.		
							Ifenprodil (3 μM; GluN2B-NMDAR antagonist) reversed enhanced eEPSC.		
							Increased Ser1303 phosphorylation of pre- and postsynaptic GluN2B. Absent in 5-HT2A KO mice.		
Rat	mPFC	DOI	3 μM		**eEPSP:** Evoked by rhythmic (0.1 Hz) electrical stimulation of the forceps minor. After DOI (10-15 min), late eEPSP appeared. Early EPSP: 5.3 mV. Late eEPSP: 9.8 mV.		Adrenaline (1-10 μM) reduced frequency and amplitude of late eEPSP. Suppression was almost complete at 10 μM. IC_{50}: 1.65 μM.	Marek & Ramos, 2018	Yes
							Adrenaline (10 μM) reduced early eEPSP amplitude up to 29%.		
							IC- 118,551 (300 nM, adrenergic β_2 antagonist) blocked the suppressant action of adrenaline.		
Mouse (WT and 5-HT2A KO)	mPFC, ACC	DOI	1 μM		**eEPSC**: Evoked by L1 stimulation. After 20 min, DOI persistently inhibited AMPAR eEPSC amplitude. 2.5 min application caused only transient depression.		Effect blocked by ketanserin (1 μM), M100907 (100 nM), NCP-15 437 (20 μM; PKC inhibitor), absent in 5-HT2A KO mice.	Berthoux et al., 2019	Yes
							Effect persisted in 4 mM Mg^{+2} and APV (50 μM; NMDAR antagonist).		
							Restoring postsynaptic 5-HT2A expression in KO mice the effect.		

							Electrically induced LTD prior to treatment occluded the effect and vice-versa. LTD was not occluded after 2.5 min DOI, with NPC-15437 (20 μM) or in 5-HT2A KO mice. Postsynaptic rescue of 5-HT2A restored the effect.		
							Preventing AMPAR internalization abolished DOI- and electrically-induced eEPSC decrease.		
							Increased phosphorylation of Ser 880 at GluA2 subunit of AMPAR. Absent after 2.5 min application, with NPC-15437 (20 μM) or GF109203X (20 μM; PKC inhibitor). Effect persisted with TTX.		
							DOI-dependent depression of AMPAR eEPSCs not prevented by AM251 (20 μM; CB1 antagonist) or anisomycin (20 μM; protein synthesis inhibitor).		
Mouse	ACC, mPFC	Psilocybin	1 mg/kg (i.p.)		**mEPSC:** 24h after psilocybin administration. Significant increase in frequency. Trend to increased amplitude (p=0.06).		Two-photon calcium imaging: Single dose of psilocybin significantly elevated dendritic density.	Shao et al., 2021	Yes
Mouse	mPFC	25CN-NBOH	0.2-10 μM		**sEPSC:** NBOH (200 nM): failed to change frequency or amplitude. NBOH (10 μM): increased frequency. The effect persisted 30 min after washout. The effect was not observed after 1h of 10 μM incubation.	**Firing frequency**: At 200 nM and 10 μM, suppression of firing evoked by two different current injection protocols. The effect persisted 30 min after washout and after 1h 10 μM NBOH incubation.	M100907 abolished the effect of 10 μM NBOH on sEPSC frequency, but failed to abolish the suppression of action potentials.	Wang et al., 2025	

					sIPSC: At 10 μM, failed to change frequency or amplitude.		XE-991 (200 nM, K_v7 inhibitor) prevented the effect of NBOH (10 μM) on firing rates.		
							Reversal potential around -60 mV and significant rheobase increase supported K_v7 involvement.		
Mouse (5-HT2A-GFP)	mPFC	Psilocin	10 μM	**Cm:** NS change	**sEPSC:** No changes in frequency or amplitude	**Firing frequency:** Without evoking stimulus, 53% of WT neurons increased firing >120% from baseline, 26% decreased firing <80% from baseline, and 21% remained unchanged.	In 5-HT2A-GFP tagged neurons, RS102221 (5 μM; 5-HT2C antagonist) decreased firing frequency. Subsequent application of psilocin or 25CN-NBOH increased firing frequency to 200% of baseline.	Schmitz et al., 2022	No
		25CN-NBOH	200 nM	**Rm:** NS change	**mEPSC:** No changes in frequency or amplitude	**Firing frequency:** In 5-HT2A-GFP-tagged neurons, firing rate significantly increased in all cells to an average of 200% over baseline.	In 5-HT2A-GFP tagged neurons, M100907 (200 nM) decreased firing frequency. Subsequent application of psilocin or -NBOH had no effect on firing frequency.		
				τ: NS change	**sIPSC:** No changes in frequency or amplitude		In 5-HT2A-GFP tagged neurons, FR900359 (1 μM; G-alpha-q inhibitor) decreased firing frequency. Subsequent application of psilocin or NBOH had no effect on firing frequency.		
							In 5-HT2A-GFP tagged neurons, psilocin significantly reduced firing frequency after postsynaptic, intracellular application of FR900359 (1 μM; G-alpha-q inhibitor).		
							In 5-HT2A-GFP tagged neurons, NBOH had no effect on firing frequency after the postsynaptic, intracellular application of FR900359 (1 μM; G-alpha-q inhibitor).		

Mouse	mPFC, ACC	25CN-NBOH	0.1-100 μM	**RMP:** No holding current. NBOH: +3-7 mV. 4-OH-DiPT: +5-7 mV. DOI: +4-3 mV.	**sEPSC**: NBOH (0.1-10 μM). Significant increase in frequency only at 10 or 100 μM treatment (+1.4 Hz in 6/11 cells and 5.6 Hz in 8/13 cells, respectively).	**Number of spikes:** Evoked by depolarizing pulse. Without holding current. Persistent decrease during 10 min NBOH (10 μM) treatment.	Intracellular delivery of NBOH (1-100 μM) produced significant decrease in firing frequency only at 10 or 100 μM, suggesting mediation of extracellular receptors.	Ekins et al., 2023	No
				RMP: 10 min time-course (NBOH, 10 μM): +5mV peak at min 4, then decays (+3 mV at min 10).	**sEPSC:** DOI treatment (10-100 μM). Significant increase in frequency. Time-dependent increase in a 10 min span.	**Firing frequency:** Evoked by depolarizing pulse. Significant, dose-dependent decrease after 10 min treatment of NBOH (0.1-100 μM), DOI (10-100 μM) and 4-OH-DiPT (100 μM).	Decrease in maximum firing frequency and F-I gain were significantly smaller following intracellular delivery of NBOH (1-100 μM) than bath application.		
		4-OH-DiPT	10-100 μM	**Ri:** NBOH 0.1-10 μM: -42% to -34% 100 μM: -12% (significant difference 0.1-10 μM vs 100 μM).	**sEPSC:** 4-OH-DiPT (10-100 μM). NS increase at 10 μM. Significant increase at 100 μM. Time-dependent increase in a 10 min span.	**Frequency-current (F-I) gain**: Evoked by depolarizing pulse. Significant, dose-dependent decrease after NBOH (0.1-100 μM).	Increase in sEPSC frequency was significantly smaller after intracellular delivery than after bath application.		
		DOI	10-100 μM	**Ri:** 4-OH-DiPT 10 μM: -27% 100 μM: +8%	**sEPSC:** 48-72h after *in vivo* DOI administration (2 mg/kg, i.p.). Significant increase in frequency. NS change in amplitude.	**Total spike output:** Evoked by depolarizing pulse. Significant, dose-dependent decrease in all treatments. Ranges: NBOH (0.1-100 Mm): -35; -76%. 4-OH-DiPT (10-100 μM): -39%; -62%. DOI (10-100 Mm): -37%; -53%.	Ketanserin abolished the effects on sEPSC but failed to abolish the effect on action potentials.		
		DOI	2 mg/kg (i.p.)	**Ri:** DOI 10 μM: -13% 100 μM: -41%			XE-991 (10 μM; K_v7 inhibitor) abolished the effect of NBOH (1-10 μM) on firing frequency and adaptation index. XE-991 abolished the effect of 100 μM NBOH on the frequency adaptation index, but not on firing frequency.		

				τ: Inconsistent variations (range: -42%; +18%)			XE-991 (10 µM) blocked NBOH (1-10 µM) -dependent decrease in maximum firing frequency and total spike output, but failed to block 100 µM NBOH.		
				Cm: Inconsistent variations (range: -8%; +12%)			XE-991 (10 µM) did not block the effect of NBOH (1-100 µM) on sEPSC.		
				All parameters: NS difference 48-72h after in vivo DOI administration (2 mg/kg, i.p.).					

Table 2: *In vivo* studies

Specie	Region	Drug	Dose	Route	Anesthesia & co-treatments	Firing	LFP	Other Findings	Reference	Peer-Review
Rat	mPFC	DOI	10 mM, 0.5-80 nA	MIO	Chloral hydrate (400 mg/kg, i.p. + i.v. as needed)	Low ejecting current (0.5 nA): DOI increased glutamate (5 nA) -induced excitation. Increased firing >20% in 11/52 cells.		$MgCl_2$ (1 M; 20-40 nA; 5-20 min) enhanced DOI's (20-80 nA) inhibition, suggesting direct action.	Ashby et al., 1989	Yes
		DOB	?		Glutamate (100 mM, 5-40 nA)	High ejecting currents (10-80 nA): DOI dose-dependently decreased glutamate (40 nA) -induced excitation. Decreased firing in all neurons		Spiperone (10 mM, 10-80 nA), metergoline (10 mM, 10-80 nA) and ritanserin (10 mM, 10-20 nA) blocked inhibition.		
						DOB acted in a similar manner.		Pindolol (10 nM, 10-80 nA), sulpiride (10 nM, 20-40 nA), and BRL-43694 (10 mM, 5-20 nA; 5-HT3 antagonist) did not affect inhibition.		
Rat	mPFC	DOI	10 mM, 10-120 nA	MIO	Chloral hydrate (400 mg/kg, i.p. + i.v. as needed)	Current-dependent firing rate suppression.		Sulpiride (10 mM, 10-40 nA) did not affect inhibition.	Ashby & Wang., 1990	Yes
								Clozapine (10 mM, 10 nA) or spiperone (10 mM, 10-120 nA) blocked inhibition.		
								Haloperidol (10 mM, 20-40 nA) potentiated inhibition.		
Rat	PFC	LSD	30-60 µg/kg	i.p.	Ketamine (80 mg/kg, i.p.)	LSD did not affect the spontaneous activity of PFC neurons.		RP 62203 (fananserin, 5-HT2A antagonist; 3 mg/kg, i.p.) co-injection abolished increased VTA-induced PFC inhibition.	Godbout et al., 1991	Yes
						LSD markedly prolonged the inhibition of PFC neurons following VTA electric stimulation.				
Rat	mPFC	DOI	10 mM, 0.5 nA	MIO	Chloral hydrate (400 mg/kg, i.p. + i.v. as needed)	Increased the firing rate of glutamate-stimulated neurons in the mPFC by 53%.		Ritanserin (unknown concentration) and 8-OH-DPAT (1 mM, 0.5-2 nA) attenuated DOI's effect.	Ashby et al., 1994	Yes
					Glutamate (10 mM, ? nA)					

Guinea pig	OFC, Head of caudate nucleus	DOI	50 mM, 5-20 pA	MIO	Chloral hydrate (200 mg/kg + 50 mg/kg/30 min, i.p.)	DOI (10 nA) suppressed quisqualate (100 nA) -induced firing in head of caudate nucleus.		Ritanserin (2 mg/kg, i.v.), metergoline (2 mg/kg, i.v.), and M100907 (1 mg/kg, i.v.) failed to block DOI (10 nA) inhibition in head of caudate nucleus.	El Mansari & Blier, 1997	Yes
					Quisqualate (1.5 mM, 90-100 nA)	DOI (30 nA) suppressed quisqualate-independent firing in OFC neurons.		Ritanserin (2 mg/kg/day, 4 days, s.c.) and metergoline (2 mg/kg/day, 4 days, s.c.) attenuated DOI (10 nA) inhibition in head of caudate nucleus.		
						DOI (5-20 nA) current-dependently suppressed quisqualate (90 nA) -induced firing in OFC. 5 nA: 30% inhibition; 10 nA: 51% inhibition; 20 nA: 90%.		Metergoline (2 mg/kg, i.v.) did not affect DOI suppression (30 nA) in OFC quisqualate-independent neurons.		
								Metergoline (2 mg/kg, i.v.) did not affect DOI suppression (10 nA) of OFC quisqualate-induced neurons (90 nA).		
								Ritanserin (2 mg/kg/day, 4 days, s.c.) or metergoline (2 mg/kg/day, 4 days, s.c.) did not affect DOI's (10 nA) inhibition of quisqualate-activated OFC neurons.		
Rat	mPFC	DOI	50 mM, 5-30 nA	MIO	Chloral hydrate (400 mg/kg, i.p. + 100 mg/kg, i.v. as needed)	Current-dependent suppression of mPFC firing.		2-7 days flibanserin pretreatment (5 mg/kg/day, s.c.; 5-HT1A agonist, 5-HT2A antagonist) reduced or abolished inhibtion.	Reuter & Blier, 1999	Yes
					Quisqualate (1.5 mM, 0-50 nA)					
Rat	mPFC, OFC	DOI	51 mM, 20-30 nA	MIO	Chloral hydrate (400 mg/kg + 50 mg/kg/30 min, i.p)	Suppressed quisqualate-induced and spontaneous firing in the mPFC and OFC.		Bicuculline (3 mM, 1 nA) had no effect in the OFC.	Bergqvist et al., 1999	Yes
					Quisqualate			Ritanserin (2 mg/kg,		

					(1.5 mM, 10 nA)			i.v.) had no effect in the OFC but suppressed inhibition in the mPFC.		
								Clozapine (1-10 mg/kg, i.v.) had no effect in the OFC, but attenuated inhibition in the mPFC.		
								Risperidone (0.1-1 mg/kg) had no effect in the OFC, but suppressed it inhibition in the mPFC.		
Mouse (WT and 5-HT2C KO)	OFC, Head of caudate nucleus	DOI	50 mM, 10-30 nA	MIO	Chloral hydrate (400 mg/kg + 100 mg/kg as needed, i.p)	DOI current-dependently inhibited quisqualate-induced firing in the OFC and the head of caudate nucleus.		M100907 (2 mg/kg, i.p.) significantly reduced OFC inhibition. Subsequent clozapine (10 mg/kg, i.p.) had no further effect.	Reuter et al., 2000	Yes
					Quisqualate (1.5 mM, 30-45 nA)	No difference between WT and 5-HT2C KO animals.		M100907 (2 mg/kg, i.p.) + clozapine (10 mg/kg, i.p.) significantly reduced head of the caudate nucleus inhibition. Post hoc analysis indicated it was not due to either M10007 or clozapine alone.		
								In 5-HT2C KO mice, neither M100907 (2 mg/kg, i.p.) nor clozapine (10 mg/kg, i.p.) reduced DOI's effects in any region.		
Rat	mPFC	DOI	0.05-0.6 mg/kg (cumulative doses)	i.v.	Chloral hydrate (400 mg/kg + 80 mg/kg as needed, i.p.)	Enhanced firing rate in 21/56 corticofugal L5/6p neurons. Firing rates increased 1525% from baseline. Mean firing rate increased 481% from baseline, due to low basal firing rates in some neurons.		Neurons typically responded to doses of 0.05–0.3 mg/kg.	Puig et al., 2003	Yes
						Firing rate of 18/56 L5/6p corticofugal neurons unaffected.		Baseline firing rates of neurons excited or inhibited by DOI were not significantly different.		
						Reduced firing rate in 17/56 L5/6p corticofugal neurons to a mean 11%.		Firing rate reductions were antagonized by M100907 (0.1-0.5 mg/kg, i.v.) and		

								picrotoxin (1-3 mg/kg, i.v.) in all cases.		
						Increased mPFC projecting neurons' output by 238%.		M100907 (0.1-0.5 mg/kg, i.v.) reversed 6/9 neurons excited.		
								LY-379268 (up to 4 mg/kg, i.v.) reversed 4/5 neurons excited.		
Rat	OFC	DOI	50 mM, 10-40 nA	MIO	Chloral hydrate (400 mg/kg. + 100 mg/kg as needed, i.p.)	Suppressed firing.		3- or 8-weeks paroxetine treatments (10 mg/kg/day, s.c.) did not affect DOI's inhibitory action.	El Mansari and Blier, 2005	Yes
					Quisqualate (1.5 mM, 10 nA)					
Rat	mPFC	DOI	0.05-0.3 mg/kg (cumulative doses)	i.v.	Chloral hydrate (400 mg/kg. + 80 mg/kg as needed, i.p.)	In corticofugal L5/6p neurons showing increased firing rates, increase in: number of spikes per burst (2 min), mean spikes per burst, burst count (2 min), burst duration, and interspike interval within bursts.	DOI reduced LFP amplitude in low frequency range (3-4 Hz) across all experiments, regardless of whether the firing rate of was increased, decreased, or unaffected.	M100907 (0.1-0.5 mg/kg, i.v.) fully reversed DOI-induced reduction in low-frequency LFP power.	Celada et al., 2008	Yes
						In corticofugal L5/6p neurons showing decreased firing rates, decrease in: spike count in bursts (2 min), burst count (2 min), burst duration, and interspike interval in bursts.		DOI reduced spike proportion during the active phase of LFP, compared to baseline, in both intact and lesioned rats. M100907 reversed this effect in both groups.		
								Haloperidol (0.1-0.2 mg/kg, i.v.) partially reduced DOI-induced LFP power reduction.		
								Clozapine (1 mg/kg, i.v.) completely reversed DOI-induced LFP power reduction.		
Mouse	vmPFC	DOI	10 mM, 5-50 nA	MIO	Chloral hydrate (400 mg/kg, i.p. + 100 mg/kg upon recovery of tail/paw pain reflexes and eye blink response)	Current-dependent firing rate inhibition.		Genetic deletion of the fatty acid amide hydrolase (FAAH; anandamide-degrading enzyme), downregulated inhibition.	Bambico et al., 2010	Yes
					Quisqualate					

					(1.5 mM, 2-5 nA)					
Rat	OFC, ACC	DOI	1-5 mg/kg	i.p.	Any. Freely moving.	In the OFC, dose-dependent decreased firing (1 to 2-fold).	In the OFC, 3 mg/kg DOI decreased low (30-55 Hz) and high (55-80 Hz) gamma band LFP power. 5 mg/kg DOI reduced low, but not high gamma power.	In the OFC and ACC, DOI decreased the correlation between spike discharge and high gamma power compared to vehicles.	Wood et al., 2012	Yes
						The number of inhibited units inhibited in the OFC was bigger than that of excited units, with the ratio increasing with dose (up to 5:1).	In the ACC, 3 mg/kg DOI reduced low, but not high gamma power. 5 mg/kg DOI reduced both low and high gamma power. Reductions in gamma power were temporally consistent and dose-dependent.			
						Response distribution significantly differed from vehicle at higher doses (3 and 5 mg/kg).				
						In the ACC, 1 mg/kg DOI caused non-significant activation in most units, with no significant difference in response distribution compared to vehicle. Larger doses (3 and 5 mg/kg) significantly suppressed firing compared to baseline in most units. At 5 mg/kg, the effect was significant compared to vehicle.				
						In the ACC and OFC, DOI dose-dependently increased the absolute value of altered firing activity (increased or decreased) above vehicle levels.				
Rat	mPFC, V1	5-MeO-DMT	1 mg/kg	i.v.	Chloral hydrate (400 mg/kg, i.p. + 50-70 mg/kg/h)	Enhanced mean firing rate of 19/37 L5/6p corticofugal neurons to 406% of baseline.	5-MeO-DMT reduced the amplitude of low-frequency oscillations (LFO, <4 Hz LFPs) in all experiments, regardless of whether the firing rate of recorded units was increased, decreased, or unaffected.	Clozapine (1 mg/kg, i.v.) and haloperidol (0.1-0.2 mg/kg, i.v.) reversed 5-MeO-DMT's effect on spike frequency and bursting.	Riga et al., 2014	Yes

					Clorgyline (0.3 mg/kg 15 min prior to 5-MeO-DMT administration)	Decreased mean firing rate of 13/37 L5/6p corticofugal neurons to 31% of baseline.	Simultaneous recordings in mPFC and V1showed 5-MeO-DMT concurrently reduced the amplitude of LFO in both areas.	Clozapine (1 mg/kg, i.v.), haloperidol (0.1-0.2 mg/kg, i.v.) and risperidone (0.2 mg/kg, i.v.) reversed the effect in LFO.		
						Mean firing rate of 5/37 L5/6p corticofugal neurons not affected.		M100907 (0.15-0.6 mg/kg, i.v.), WAY1006635 (25-100 ug/kg, i.v.; 5-HT1A antagonist) and LY-379628 (0.5-2 mg/kg, i.v.; mGlu2/3 agonist) reversed the effect in LFO.		
						Overall corticofugal L5/6p mean firing rate increased to 215% of baseline.		LY-379628 (0.5-2 mg/kg, i.v.) alone induced a slight, but significant and dose-dependent increase in LFO power (104-135%).		
						Significant increase in the number of spike bursts in 2 min.		Significant reduction in BOLD fMRI signal in mPFC and V1. No significant changes in PaCO2 or PaO2 accounted for this.		
Mouse (WT and 5-HT2A KO)	mPFC, S1, Au1, V1	5-MeO-DMT	1 mg/kg	s.c.	Chloral hydrate (400 mg/kg + 50-70 mg/kg/h, i.p.)		Reduced LFO power in the mPFC of WT mice (51% of baseline) and 5-HT2A KO mice (61% of baseline). The effect of genotype was significant.	Pretreatment with WAY-100635 (5-HT1A antagonist, 0.5 mg/kg, s.c.) fully prevented 5-MeO-DMT's reduction of LFO in the mPFC of 5-HT2A KO mice.	Riga et al., 2016	Yes
							In 5-HT2A KO mice, mPFC LFO reduction after 12 min (61% of baseline) was significantly bigger than after 24 min (75% of baseline). In WT mice, any significant difference was observed.	Risperidone (1 mg/kg, s.c.) or haloperidol (0.6 mg/kg, s.c.) attenuated the effect of 5-MeO-DMT on mPFC LFO power.		
								5-MeO-DMT reduced ECoG LFO in S1, Au1 and V1 of WT mice, but not in S1 and Au1 of 5-HT2A KO mice.		

Mouse (WT and 5-HT2A KO)	mPFC, V1, thalamus (MD)	5-MeO-DMT	5 mg/kg	s.c.	Any. Freely moving.		In WT mice, increased theta (4-10 Hz) and gamma (30-80 Hz) power in the mPFC and delta (0.2-4 Hz) power in V1. In MD, beta power was decreased. Cortical effects were more pronounced than thalamic effects.	In WT mice, pretreatment with risperidone (1 mg/kg, s.c.) only prevented 5-MeO-DMT effect in mPFC theta band and in mPFC-MD coherence.	Riga et al., 2018	Yes
							In WT mice, increased mPFC-V1 coherence in the beta (10-30 Hz) band, mPFC-MD coherence in theta and beta bands, and V1-MD coherence in beta band.	In 5-HT2A KO mice, pretreatment with WAY-100635 (0.5 mg/kg, s.c.) prevented all 5-MeO-DMT effects in LFP power and coherence, except in delta V1-MD coherence.		
							In 5-HT2A KO mice, increased power in all examined bands in the mPFC. Increased delta, theta and beta in V1, and increased delta in MD.			
							In 5-HT2A KO mice, increased mPFC-V1 coherence in theta and beta bands, mPFC-MD coherence in delta, theta and beta bands, and V1-MD coherence in delta and beta bands.			
Mouse	mPFC, HPC	DOI	1 mg/kg	i.p.	Any. Freely moving.	Modest decrease in multi unit activity (MUA) in the mPFC.	Selective enhancement in LFP high gamma power (50-100 Hz).	Enhanced PFC-HPC high gamma phase synchronization	Gener et al., 2019	Yes
								M100907 (1 mg/kg, i.p.) reversed DOI's effect on LFP and PFC-HPC synchronization.		
								A smaller dose of DOI (0.3 mg/kg, i.p.) exerted similar effects.		
								DOI reversed risperidone (2 mg/kg, i.p.) -mediated decreases in beta and gamma LFP in PFC and HPC, and		

								normalized delta increases in PFC. Risperidone-reduced MUA and theta oscillations persisted.		
Rat	IL/PL PFC, thalamus	DOI	1 mg/kg	s.c.	Any. Freely moving.		In the right mPFC, significant suppression in theta (4-10 Hz) power occurs only in the inactive state.	Suppression of delta activity in thalamic LFP and ECoG (inactive state).	Hansen et al., 2019	Yes
							DOI did not significantly affect low (30-60 Hz) or high (60-100 Hz) gamma activity. In all recorded regions, there was a trend towards decreased power in the low gamma band in both states. High gamma suppression trends were observed only in the inactive state.	Suppression of theta power in thalamic LFP and ECoG (inactive state).		
							DOI enhanced HFO (130-160 Hz) in mPFC during locomotion and in all areas during inactivity.	Suppression of beta power in thalamic LFP and ECoG (inactive state).		
								Effects on HFOs were significantly higher during inactivity than locomotion.		
Mouse (WT and Raptor KO)	PL and IL vmPFC	LSD	Acute: single dose of 30 µg/kg	i.p.	Urethane (1.4 g/kg, i.p.)	Basal firing rates were unchanged after acute or chronic LSD.		Chronic LSD enhanced the current-dependent excitatory effect of local quisqualate (1.5 mM, 20-50 nA). Firing rates increased to 250-300%.	De Gregorio et al., 2021	Yes
			Chronic: 30 µg/kg/day, 7 days	i.p.	NMDA (50 mM, 5 nA)	The number of spikes per burst firing was increased after chronic LSD.		Chronic LSD did not affect the current-dependent excitatory effect of local NMDA (50 mM, 20-50 nA).		
		DOI	10 mM, 20-50 nA	MIO		Local DOI treatment current-dependently increased basal firing rates (175-200%).		Chronic LSD did not affect the current-dependent inhibitory effect of local 8-OH-DPAT (50 mM, 20-50 nA).		
						Chronic LSD enhanced the current-dependent excitatory		In Raptor (adaptor protein in mTORC1) KO		

						effect of local DOI (firing rates increased to 200-300%)		mice, the potentiation of local DOI or quisqualate by chronic LSD is significantly attenuated.		
Mouse	IL PFC, thalamus (MD and Reticular)	LSD	5-160 μM	i.p.	Urethane (1.2 g/kg, i.p. + 0.12 g/kg as needed)	In the PFC, increased firing frequency (+15%) in 4/5 pyramidal neurons only at the highest (160 μg/kg) dose. 1/5 neurons not affected. Any changes in burst firing.		Haloperidol (150 μg/kg, i.p.) 10 min after LSD (160 μg/kg) increased burst activity in reticular neurons inhibited by LSD, and rescued the disinhibition of MD neurons.	Inserra et al., 2021	Yes
						In the MD thalamus, increased firing frequency (+15% baseline) and number of bursts in 100s from at 40 μg/kg dose and above, in all relay neurons tested.				
						In the reticular thalamus, 7/14 GABAergic neurons increased firing frequency (+15% baseline) at ⩾ 80 μg/kg, and bursts in 100s at ⩾ 40 μg/kg.				
						In the reticular thalamus, 7/14 GABAergic neurons decreased firing frequency (-15%) at ⩾ 20 μg/kg, bursts in 100s at ⩾ 10 μg/kg, and % of spikes in bursts at ⩾ 10 μg/kg.				
Mouse	IL/PL PFC, ACC	Psilocin	2 mg/kg	i.p.	Any. Freely moving.		In both wake conditions (undisturbed and sleep-deprived), baseline spectra from frontal EEG and LFP showed a peak around 4 Hz. This power enhancement (3-5 Hz) was reduced in sleep deprivation conditions in LFP.	The power enhancement around 3-5 Hz in frontal EEG showed a negative correlation with electromyography variance. Additionally, it had been associated with a quiet, restful state.	Thomas et al., 2022	Yes
							In wake animals, gamma power >60 Hz was enhanced during the sleep deprivation condition.	In both wake conditions, there was a widening in theta peak (5-8 Hz) in the occipital EEG.		
							During NREM sleep, no clear differences were identified, but a trend	In wake conditions, gamma power (>30 Hz) was generally		

							showed decreased frequencies <4 Hz in LFP and all EEG signals, possibly indicating more shallow sleep.	decreased in both EEG derivations and to a greater extent in the undisturbed condition.		
							During REM sleep, high frequencies (>30 Hz) tended to be reduced while low frequencies (>8 Hz and 10-20 Hz) were mostly increased. This might reflect bleeding of NREM features to REM sleep.	In animals treated with psilocin, the first attempts to sleep failed and many stayed in restful positions compatible with sleep although they stayed awake.		
Rat	OlfC, OFC, mPFC, TAA, SMC, vStr, dStr, Integrative Thalamus, Associative Thalamus, Sensory Thalamus	DOI	2 mg/kg	i.p.	Any. Freely moving.	Across all regions, 65% of neurons were inhibited, and 8% were excited by DOI or LSD.	In the OFC and the mPFC, LSD and DOI increased the power of high frequency oscillations (HFO) in the LFP spectrum between 100 and 150 Hz.	The inhibition of pyramidal cells from the TAA was significant after both LSD and DOI treatments (z-scores to baseline around -05 and -0.3, respectively).	Brys et al., 2023	Yes
	Cortical layers not specified.	LSD	0.3 mg/kg	i.p.		In all recorded regions, DOI and LSD predominantly caused inhibition. This applied to both principal cells and interneurons.	LSD and DOI increased the prevalence of HFOs in the OFC and mPFC.	In the TAA, the fractions of inhibited principal cells were significant after both LSD and DOI treatments.		
						In the mPFC, LSD significantly reduced firing of principal and non-identified cells (z-score <-0.75 to baseline).		LSD and DOI also increased HFO power in the OlfC, SM cortex and vStr.		
						In the mPFC, DOI did not		LSD and DOI increased		

						significantly affect the firing of any cell type.		HFO prevalence in the OlfC, dStr, and vStrs, with the most persistent effect in the vStrs.		
						In the OFC, LSD significantly increased the fraction of inhibited principal cells and interneurons.		During the psychedelic state, 37% of cells showed HFO-entrained spiking, a significant increase from 28% at baseline.		
						In the mPFC, LSD significantly increased the fraction of inhibited principal cells, interneurons and non-identified neurons.		All cell types showed a clear preference for phases around 2 rad before the HFO.		
						In the OFC, DOI significantly increased the fraction of inhibited principal cells and interneurons.		Entrainment strength (mean kappa) was modestly increased during the psychedelic state compared to baseline. Principal neurons in the vStr showed the strongest entrainment (mean kappa = 0.27), while principal cells in the TAA were also strongly entrained (mean kappa = 0.24), despite modest HFO power in this region.		
						In the mPFC, DOI did not change in the fraction of inhibited cells significantly.		Phase-synchronized HFOs in regions including the olfactory bulb, OlfC, OFC, mPFC, and vStr showed near-zero phase lags, inconsistent with a single source propagating synaptically or via volume transmission. Phase inversions in adjacent electrode measurements suggest HFOs are generated by a system of several self-sustaining, weakly interacting oscillators.		

								Structure-by-structure analysis showed that Granger causality was strongest from vStr to mPFC, indicating a strong influence of the former on the latter.		
Rat	OlfC, OFC, PFC, SMC, TAA, dStr, vStr, Sensory Thalamus, Integrative Thalamus, Septal Area	LSD	0.3 mg/kg	i.p.	Any. Freely moving.		The average broadband LFP power spectrum was weakly decreased, suggesting reduced neuronal firing, but none of the nine structures showed significant changes compared to baseline.	There was a significant decrease in functional connectivity within structures and a non-significant decrease in functional connectivity between structures.	Nasretdinov et al., 2023	Yes
							Slope flattening in the broadband LFP power spectrum suggested a significant E-I shift towards excitation in local circuits of the OFC, PFC, and SMC			
							Slope steepening in broadband LFP power spectrum suggested a significant E-I shift towards inhibition in the TAA.			
Rat	mPFC, HPC	5-MeO-DMT	1-10 mg	i.p.	Any. Freely moving.		In the mPFC, i.p. injection led to dose-dependent increase in delta (1-4 Hz) and theta (5-12 Hz) power, while ICV injection led to dose-dependent decrease of theta power.	State maps based on LFP power ratios showed that 5-MeO-DMT pushed the HPC activity closer to the states observed during baseline sleep despite animals being awake (either after i.p. or ICV injection).	Souza et al., 2024	Yes
			100-200 µg	ICV			In the HPC, dose-dependent increase in delta power following i.p. injection, and decrease in theta power following both i.p. and	Locomotor activity was taken into consideration as a confounding factor.		

							ICV injections.			
							In the HPC, decrease in slow (20-50 Hz) and mid (50-100 Hz) gamma power when nested in theta cycles, and decreased theta modulation of slow gamma oscillations, specifically following ICV injection.			
Mouse	ACC, premotor mPFC	Psilocybin	1 mg/kg	i.p.	Any. Head fixed.	16% of PT (see notes) neurons substantially increased spiking activity (Z>2), while 2% were substantially inhibited (Z<-2).		Calcium imaging showed that psilocybin preferentially boosts Ca^{2+} transients in apical dendrites of PT over IT neurons.	Shao et al., 2025	Yes
						3% of IT (see notes) neurons substantially increased spiking activity (Z>2), while 0% were substantially inhibited (Z<-2)				
						On average, the firing rate increased significantly over baseline in PT neurons, but not in IT neurons.				
Mouse		TCB-2	0.15-0.5 mg	p.o.	Any. Head fixed.	39% of all neurons increased firing rates. 11% showed >2-fold increase in fitted step function.	Reduced beta and low gamma power by 20%.		Dearnley et al., 2021	No
						61% of all neurons decreased firing rates. 21% showed >2-fold decrease in fitted step function. Significant compared to vehicle (5% decrease).	Small, significant increase in high gamma (around 64 Hz) power.		Dearnley et al., 2023	Yes
						Mean firing log-rate decreased significantly compared to baseline (0.36 vs 0.25) and control (0.37 vs. 0.25).			Dearnley, 2023	PhD Thesis
						Log-rate distribution was stretched leftward and standard deviation increased significantly.				
						Despite prominent log-rate change, total spike count remained stable.				
						TCB-2 dose significantly				

						correlated with log-rate distribution stretching.				
						Increased distance in log-rate distribution of excited (39%) and inhibited (61%) neurons. Shifts to the left accompanied by increased dispersion. Shifts to the right reduced dispersion.				
						In upregulated neurons, firing rate modulation was negatively correlated with baseline log-rate; the opposite was true for downregulated neurons.				

Microiontophoretic ejecting currents are expressed in absolute value.

CM: Centromedial thalamic nucleus, IL: Infralimbic, IT: Intratelencephalic neurons, HPC: Hippocampus, MD: Mediodorsal thalamic nucleus, MIO: Microiontophoresis, OFC: Orbitofrontal cortex, OlfC: Olfactory cortex, PL: Prelimbic, PT: Pyramidal tract neurons, SMC: Somatosensory cortex, dStr/vStr: Dorsal/ventral striatum, TAA: Temporal association area.